Summer 2010

Exploration of TRPV1 Splice Variant Expression in Rat Dorsal Root Ganglia Following Sciatic Nerve Injury

Karl A. Andersen

EXPLORATION OF TRPV1 SPLICE VARIANT EXPRESSION IN RAT DORSAL ROOT GANGLIA FOLLOWING SCIATIC NERVE INJURY

A Thesis

Submitted to the Bayer School of Natural and

Environmental Sciences

Duquesne University

In partial fulfillment of the requirements for

the degree of Master of Science

By

Karl Andersen

August 2010

EXPLORATION OF TRPV1 SPLICE VARIANT EXPRESSION IN RAT DORSAL ROOT GANGLIA FOLLOWING SCIATIC NERVE INJURY

By

Karl Andersen

Approved June 23, 2010

_____	_____
John A. Pollock, Ph.D. Associate Professor of Biology (Thesis Director)	Brady Porter, Ph.D. Associate Professor of Biology (Committee Member)
_____	_____
David L. Somers, Ph.D., PT Chair, Associate Professor, Department of Physical Therapy (Committee Member)	Michael Jensen-Seaman, Ph.D. Assistant Professor of Biology (Committee Member)
_____	_____
David W. Seybert, Ph.D. Dean, Bayer School of Natural and Environmental Sciences	Philip E. Auron, Ph.D. Chair, Professor, Department of Biological Sciences

ABSTRACT

EXPLORATION OF TRPV1 SPLICE VARIANT EXPRESSION IN RAT DORSAL ROOT GANGLIA FOLLOWING SCIATIC NERVE INJURY

By

Karl Andersen

August 2010

Thesis supervised by John A. Pollock, Ph.D.

Transient Receptor Potential Vanilloid 1 (TRPV1) is ligand-gated ion channel that plays an important role in the pain signaling pathway. It is predominantly expressed by sensory neurons located in trigeminal ganglia or dorsal root ganglia (DRG). TRPV1 has been shown to play a crucial role in the generation and maintenance of inflammatory and neuropathic pain. The involvement of splice variants of TRPV1 in pain pathways is not well known. In this study, the mRNA expression of TRPV1 and 3 splice variants (TRPV1.b, TRPV1.β, and TRPV1.var) in DRG was measured following chronic constriction injury of the sciatic nerve in rats. This is the first study to isolate TRPV1.β in rat DRG. The expression of TRPV1 mRNA was elevated following peripheral nerve damage, but not TRPV1.b, TRPV1.var or TRPV1.β. These novel findings suggest that the expression of TRPV1 splice variants is not regulated by sciatic nerve injury.

ACKNOWLEDGEMENTS

I would like to thank Dr. John A. Pollock, my thesis advisor, for giving me the opportunity to work on this fascinating, maddening, and fun project. During my time in his lab, I learned to work independently and creatively, be resourceful, make mistakes and learn from them, and really appreciate the complexity and beauty of science. To my committee members, Dr. David Somers, Dr. Brady Porter, and Dr. Michael Seaman, I thank you for guidance, instruction, and patience. I have greatly appreciated the opportunity to work with all of you. I would like to thank Dr. Somers for graciously taking time out of his busy life to teach me how to perform the necessary behavioral tests and surgeries for this project. Dr. Somers' feedback and comments also really helped me to think critically about the project and elevate the level of science I was conducting. Many thanks to Dr. Sarah Woodley for her help with the statistical analysis and figure construction. I want to thank Dr. Seaman and his entire lab for their assistance and patience with my unannounced visits. I thank Mr. Robert Hoggard for his beautifully rendered rat anatomy drawings, which help detail the CCI surgery. To all of my past lab members, you have my graditude: Mrs. Bree Zeyzus Johns, Ms. Candice Kruth, Mr. Jordan VerPlank, and Mr. Alex Ruiz. I would especially like to thank Bree for being the first to tackle this project. She cleared the path for my work, and without her guidance, I quickly would have gotten lost. I would like to thank my fellow Biology graduate students, many of whom have become close friends. Many thanks to Duquesne University, the Bayer school, and the Department of Biology, which gave me the opportunity to switch to the Master's with thesis program. To my parents, Arnold and

Helen Andersen, I am incredibly grateful for the support, encouragement, and opportunities that they have given to me. They helped foster my curiosity and love for biology for as long as I can recall. But of all the people that I am thankful for, I am most thankful for my wife, Carly Andersen. During the past three years, she has been my source of strength, joy, and happiness. I am incredibly blessed to have her in my life.

TABLE OF CONTENTS

Page

LIST OF TABLES

Page

LIST OF FIGURES

Page

Chapter 1

INTRODUCTION

Pain and its consequences

According to the International Association for the Study of Pain (IASP), pain is defined as, "an unpleasant sensory and emotional experience associated with actual or potential tissue damage, or described in terms of such damage" [1] As implied by the definition, pain is a phenomenon that eludes easy classification. It is shared among all humans and with most metazoan species in some form or another, but manifests in a myriad of ways. One may experience pain in response to jamming a toe, touching a hot stove, or eating an ice cream sundae too quickly. And at the same time, athletes and soldiers have reported feeling no pain following severe trauma, such as when a football player breaks a finger while running down field or when a soldier is wounded on the battlefield. Understanding how our bodies generate and transmit painful signals is becoming one of the greatest challenges of modern medicine.

Researchers studying pain divide it into two broad categories: acute and chronic [2]. Acute pain is the type of pain that is associated with a diagnosable source, such as trauma, injury, or surgery. . In most cases, acute pain has a defined period of time: usually the time it takes the body to heal itself. And, acute pain can be relatively well controlled with medicines. Chronic pain is a pain that persists, sometimes long after the

original injury has healed. It can arise from a variety of sources, including cancer, arthritis, arachnoiditis (inflammation of the arachnoid membrane), and those are just a few of the diseases that have known etiologies. Some diseases, such as fibromyalgia or complex regional pain syndrome, have no well-defined origins. Sufferers of chronic pain often experience diminished quality of life and relationships, and are more likely to suffer from depression as a consequence [3].

Extending beyond the suffering of the individual, pain has a serious effect on society. Pain is a significant contributor to decreased work productivity, lost worker hours, and work performance. In 2003, a study by Stewart et al. [4] found that common painful conditions, such as arthritis, migraines, back pain, and other musculoskeletal afflictions, resulted in the loss of $61.2 billion per year, and affected 13% of the total workforce during a two-week period. Additionally, this study did not include other types of pain such as dental pain, cancer pain, neuropathy, or pain associated with menstruation. Kathryn Weiner, director of the American Academy of Pain Management went so far as to say that pain is an epidemic in America [5]. She points out that in 1999, 4 out 10 people responding to a survey were unable to obtain adequate pain management therapies for moderate to severe pain. The cost of pain is expected to rise as a consequence of people working longer, and the estimated 75 million American baby boomers increasing in age.

Currently, the common pharmacological solutions to alleviating pain and, in particular, chronic pain, are not always effective. Unlike other diseases, which can have targeted solutions, pain is treated in a nonspecific manner, usually relying on non-steroidal anti-inflammatory drugs (NSAIDS), or opiods, such as morphine or codeine, to

control symptoms. A consequence of these drugs freely circulating and interacting with various regions of our bodies is that they can have serious side effects [6]. The NSAIDs, such as acetominophen and ibuprofen, diminish mild to moderate pain by inhibiting cyclooxygenase (COX) enzymes, COX-1 and COX-2, throughout the body. These two enzymes synthesize inflammatory molecules including prostaglandins, among others. Opiods create an analgesic effect by binding to opiod receptors within the central nervous system. Though very effective at dulling the experience of moderate to severe pain, opiods have many side effects, ranging from mild to severe, including constipation, disorientation, and respiratory depression. The continued usage of opiods can also lead to dependency and decreased efficiency, due to tolerance of the drugs. Opiods also have a greater potential for abuse and misuse [7,8,9].

Long-term, non-dependent, and effective pain management therapies are likely to increase in importance as more people suffer from chronic pain, especially since the current drugs are not adequately solving the problem [10, 11]. The key to cracking the problem of chronic pain will come from a greater understanding how painful stimuli are recognized, propagated, integrated, and interpreted as pain. One of the goals of this project is to expand our understanding of the molecular basis for pain circuitry, which will allow us to disrupt it with fewer adverse consequences.

How we feel pain

Like hunger, sleep, and thirst, pain is a powerful behavioral motivator. It has the power to compel us to act, often in ways that are far different from our normal routine. In a sense, it is the body's alarm system. It alerts us to possible damage to our bodies, and compels us to stop what we were doing, or to seek medical help if necessary. Though we

now experience it in a multimodal, multifaceted way, pain first evolved as a simple protective mechanism, a way for the body to inform the brain that it has experienced harm of some sort, be it inflammation, injury, or trauma.

The actual sensation of pain originates at the peripheral terminals of primary afferent pain fibers, which are located in the skin and viscera. They are responsible for monitoring the chemical, thermal and mechanical environment. These specialized nerves were given the name nociceptors by Charles Sherrington at the beginning of the 20th century [12,13]. They are unique among somatosensory neurons in that they respond to the same stimuli as all other neurons, but their threshold of activation is much higher [14]. Their sensory specification is also due to their possession of unique combinations of ion channels that are tuned to respond to only noxious stimuli. Following activation at the nerve terminal, noxious signals are sent back to the cell body, which are largely located within dorsal root ganglia or trigeminal ganglia, and then to the central terminal, which is the interface between the central and peripheral nervous systems. At the central terminal, the nociceptors form synapses with second order neurons in discrete regions of the dorsal horn, primarily within lamina I and II [15]. The signal is transferred from the ganglia to the central terminal in the form of neurotransmitters and neuropeptides, including, among others, substance P, Calcitonin gene-related peptide, and neuropeptide tyrosine [15]. From there, the noxious signals are relayed to discrete regions of the brain that are responsible for interpreting the signal as painful.

The Transient Receptor Potential Superfamily

Currently, there are 28 known mammalian members of the Transient Receptor Potential (TRP) protein channel superfamily. They are divided into 6 sub-families. The original TRP was defined by a physiological phenotype of a transient receptor potential in the electroretinograms of *Drosophila melanogaster* strains that had been chemically mutagenized [16]. Later work by Baruch Minke showed that the TRP protein played an intermediate role between photoreception and the opening of light-sensitive channels (Minke, 1982, Montell and Rubin). In 1989 the *trp* locus was cloned from *Drosophila* and shown to have sequence similarity to Ca^{2+} channel genes [17].
Classification of the mammalian TRP proteins was decided on by the TRP Nomenclature committee in 2002 [18]. Members of the TRPC subfamily were named such because they are the ones that most closely resemble the first TRP gene isolated from *Drosophila* [19]. These members are termed "canonical" TRPs based on sequence homology. The other five subfamilies are named after the first protein of that subfamily that was defined. The TRPV1 subfamily was named after the vanilloid receptor 1. The TRPM subfamily was named after melastatin, which is a predicted tumor suppressor gene [20]. TRPML was named after the protein mucolipin, which, when mutated, causes the disease Mucolipidosis type IV [21, 22]. The TRPA subfamily was named after its founder gene ankyrin-like with transmembrane domains 1 (ANKTM1) [23]. TRPP was named after polycystin-1, which when mutated, causes the disease autosomal dominant polycystic kidney disease (ADPKD) [19, 24].

Structurally, all TRP channels are similar, sharing six transmembrane domains, a pore-loop between the fifth and sixth domains, and cytoplasmic NH_2 and COOH termini

[25]. Almost all are calcium-permeable cation channels [26]. TRP channels respond to a wide array of stimuli, including heat, cold, osmotic stress, pH changes, and a wide variety of chemicals, including menthol, allicin, mustard oils, and even jellyfish toxins [27,28,29,30]. TRP channels also act as taste receptors and contribute to the detection of bitter, sweet, and umami [31]. TRPs relay information back to the soma by altering Ca^{++} concentrations, either by directly permitting its entrance into the cell, or by allowing other cations into the cell that then activate pathways to release Ca^{++} from internal stores. This flux of Ca^{++} ions causes the cell to become depolarized and result in an action potential, informing the brain of the painful stimuli [19]. Like other channels, members of the TRP family are known to form heterotetramers or homotetramers, depending on the specific protein, which allows the complex to be more sensitive to specific stimuli and be more selective of which cation passes through [32]. Normally, the channels are homotetramers, but a few cases of heteromerization between proteins, such as between TRPV1 and TRPA1, and TRPV1 and TRPV2, have been reported [10, 33].

Within this diverse superfamily, a subset of the proteins are involved in the transduction of painful or noxious stimuli. These pain-sensing TRPs are TRPM8, TRPA1, and TRPV1-TRPV4. These proteins are often referred to as ThermoTRPs since they are partially responsible for sensing different temperatures. The vanilloid TRPs sense warm to painfully hot temperatures, and TRPM8 and TRPA1 are involved in sensing cool and cold temperatures [30, 34].

Transient Receptor Potential Vanilloid 1 (TRPV1)

Of the known pain transducing TRPs, the best understood one is Transient Receptor Potential Vanilloid 1 (TRPV1), a member of the vanilloid subfamily of the TRP

superfamily. First cloned and described by Caterina et al. in 1997 [35], TRPV1 is perhaps best known as the capsaicin receptor. Capsaicin is a small, vanilloid molecule responsible for the spicy flavor of chili peppers. TRPV1, however, responds to more than just capsaicin, as it is a polymodal nociceptor, and can integrate multiple additional stimuli including noxious heat detection (≥43°C), protons, low pH, certain jellyfish and spider toxins, camphor, and allicin (a pungent molecule found in onions and garlic) [28, 36, 37]. The channel is also sensitized by a whole host of intracellular molecules, including bradykinin, nerve growth factor, prostaglandins, ATP, calmodulin, anandamine, diacylglycerol, and eicosanoids [38, 39, 40, 41]. Most of these molecules sensitize TRPV1 by directly or indirectly phosphorylating the protein [42]. Sensitization of TRPV1 can lower the thermal threshold to normal body temperatures [43], contributing to thermal hyperalgesia, a symptom of chronic pain states.

TRPV1 is primarily expressed in capsaicin-sensitive bipolar neurons whose somata are most often located in dorsal root ganglia (DRG) or trigeminal ganglia [42, 44]. This subpopulation of primary afferent neurons are usually lightly myelinated (Aδ fibers) or unmyelinated (C fibers) [41, 45]. TRPV1 expression is not limited to neurons innervating the skin or musculoskeletal system, and has been identified in neurons innervating the urinary tract [46,47], the cardiovascular system [48,49], and the mucous membranes of the mouth and esophagus [35]. The presence of TRPV1 has also been confirmed in the CNS, including the hypothalamus and substantia nigra [50,51]. The expression of TRPV1 in non-neuronal tissue is far lower than in neuronal tissue [52]. Like other TRP channels, TRPV1 is an ion channel, and is relatively selective for Ca^{++} and Mg^{++} [43].

The role of TRPV1 as a nociceptor has been widely documented in a variety of different acute, chronic, and neuropathic pain models and diseases. Earlier studies have shown that capsaicin alone can cause hyperalgesia (the reduction of pain thresholds) and pain-like symptoms in animals and humans [53,54]. TRPV1 has also been shown to be associated with painful diseases such as diabetic neuropathy, chronic pancreatitis, cancer pain, osteoarthiritis, and gastrointestinal diseases [55,56,57,58,59]. The role of TRPV1 as a nociceptor has also been demonstrated with TRPV1 knockout mice [60,61]. These *trpv1*$^{-/-}$ mice display normal responses to noxious heat, but do not experience the same amount of hyperalgesia that usually accompanies inflammatory pain [60].

In the past 10 years, many studies have been conducted to determine if TRPV1 expression is altered by disease or injury. In a study of rats having received partial sciatic nerve ligation, or lumbar level 5 spinal nerve ligation, TRPV1 protein expression was elevated in uninjured DRG somata [62]. In the spine, TRPV1 levels have also been shown to be elevated in expression following sciatic nerve injury [63]. In cervical DRG, TRPV1 expression was also increased, following the administration of complete Freund's adjuvant to the forepaws of rats [64]. While numerous sources demonstrate that TRPV1 protein levels increase via immunohistochemistry or western blotting, fewer sources show that disease or pain models induce an increase in TRPV1 mRNA expression in DRG tissue. A study using a peripheral nerve injury model found that mRNA for TRPA1, TRPM8, and TRPV2 increased in DRG tissue, but not TRPV1. Another study that measured TRPV1 mRNA levels in DRG tissue using an oligonucleotide probe (complementary to bases 2581–2625 of rat V1 sequence) found that TRPV1 levels increased in lumbar level 4 (L4) and decreased in L5 following a different nerve injury

model [65]. A possible explanation for the discrepancy between the expression differences of TRPV1 protein and mRNA is that not all mRNA studies conducted tissue specific analyses. The contribution of nerves to the sciatic nerve is not equal between DRG levels, so one would not expect to see equal changes in TRPV1 mRNA expression in the soma of these different tissue samples. Furthermore, the combination of RNA from different DRGs would diminish apparent TRP mRNA expression since any increase found in one specific tissue would be diluted by the addition of RNA from the other tissues. Bree Zeyzus, a former graduate student of the Pollock Lab, sought to shed light on this problem by performing a study where she analyzed TRPV1 mRNA expression in a tissue specific manner following induction of chronic pain [66].

Splice variants of TRPV1

The second focus of this research project was to determine the contribution of alternatively spliced variants of the TRPV1 gene to nocioceptive pathways. Put simply, splice variants are different mRNAs produced from the same gene. The mRNAs will produce protein isoforms that have a different amino acid composition from the canonical form, and consequently may have different roles or functions within the cell. This violation of the dogma "one gene, one protein" allows organisms to economically generate a larger proteome without having to maintain extra genes. These additional peptides can have different ligand binding properties, allosteric properties, or enzymyatic activity [67]. Reliance on alternative splicing to generate novel polypeptides instead of genes, however, makes organisms more susceptible to problems if the alternative splicing mechanism is disrupted. In the brain, for example, the Tau splice isoforms are involved in microtubule formation and stabilization. Errors in the alternative splicing of Tau

contribute to neuropathologies such as Alzheimer's disease [68]. One example of expression being regulated by alternative splicing is that variant mRNA transcripts can be created in order to generate a premature termination codon that targets the transcript to be destroyed via the nonsense-mediated decay pathway rather than turned into proteins [69]. This process can serve as an additional check-point to halt the expression of functional proteins. In the case of TRPV1, splice variants may serve to modulate the sensitivity and activity of the mature channel [70]; act as dominant negative regulators [71], altering the expression of mature channels; and serve non-nociceptive purposes, such as detecting salts in taste receptor cells [72].

The process that produces splice variants is called alternative splicing of pre-mRNA. Inside the nucleus, alternative splicing begins with the transcription of DNA into RNA. The large enzyme complex, RNA polymerase II, faithfully copies the entire TRPV1 gene sequence, including both exons and introns. Exons are smaller DNA segments within the gene sequence that contain the instructions for amino acid synthesis. The introns are generally larger segments of DNA that intervene between the exons and contain regulatory elements or unknown elements. After transcription has occurred, the pre-mRNA molecule typically undergoes a series of modifications that include the addition of the 7-methylguanosine cap to the 5' end of the primary transcript, polyadenylation of the 3' end, and the removal of introns, which are not needed for translation. The removal of introns is a complicated process called mRNA splicing, and is carried out by a ribonucleoprotein complex called the spliceosome. The spliceosome is one of the largest complexes in the cell, consisting of over 200 proteins and at least 5 small nuclear RNA molecules [73]. The spliceosome's ability to distinguish exons from

introns is not completely understood, but the two major contributing components are splice site consensus sequences and flanking regulatory regions called intronic or exonic splicing enhancers or silencers [74]. Splice site consensus sequences are conserved recognition sites for the spliceosome situated at exon/intron borders [67,75]. There are unique consensus sequences at the start and finish of intronic sequences; the beginning of an intron almost always begins with the nucleotides GU and ends with the nucleotides AG. Exonic and intronic splice site enchancers or silencers help mediate the splicing process by serving as binding sites for proteins that guide or repel the spliceosome subunits from assembling at nearby splice sites [74].

One reason that alternative splicing is such an important and powerful process is that it is not uniform in its occurrence. The same gene can undergo alternative splicing in a tissue-dependent or developmental-dependent manner allowing for very precise regulation to be maintained throughout the body, and over time. One famous example of alternative splicing occurs during the sex-determination process in *Drosophila melanogaster*. The protein Sex lethal is only expressed in female cells, and it suppresses certain splicing patterns of pre-mRNA transcripts that would lead to male development [67]. The pattern of alternative splicing is also not uniform as one gene can have many different splicing combinations, allowing for hundreds or thousands of different isoforms. Currently, the *Drosophila* gene Down syndrome cell-adhesion molecule (Dscam) is the leader, with a possible 38,016 different isoforms [75].

Since its initial discovery, many different forms of alternative splicing have been identified (Figure 1). The different types of alternative splicing include retained introns, alternative 3’ or 5’ splice sites, alternative translational start sites, cassette exons (entire

exons that are removed), and mutually exclusive exons, among other types. See for examples of alternative splicing. Alternative splicing was once thought to be a relatively rare phenomenon, but recent analyses have suggested that anywhere from 60-90% of all human genes undergo alternative splicing [76]. This finding reconciles the difference between the >100,000 observed unique polypeptides and the 20,000-25,000 known genes in humans.

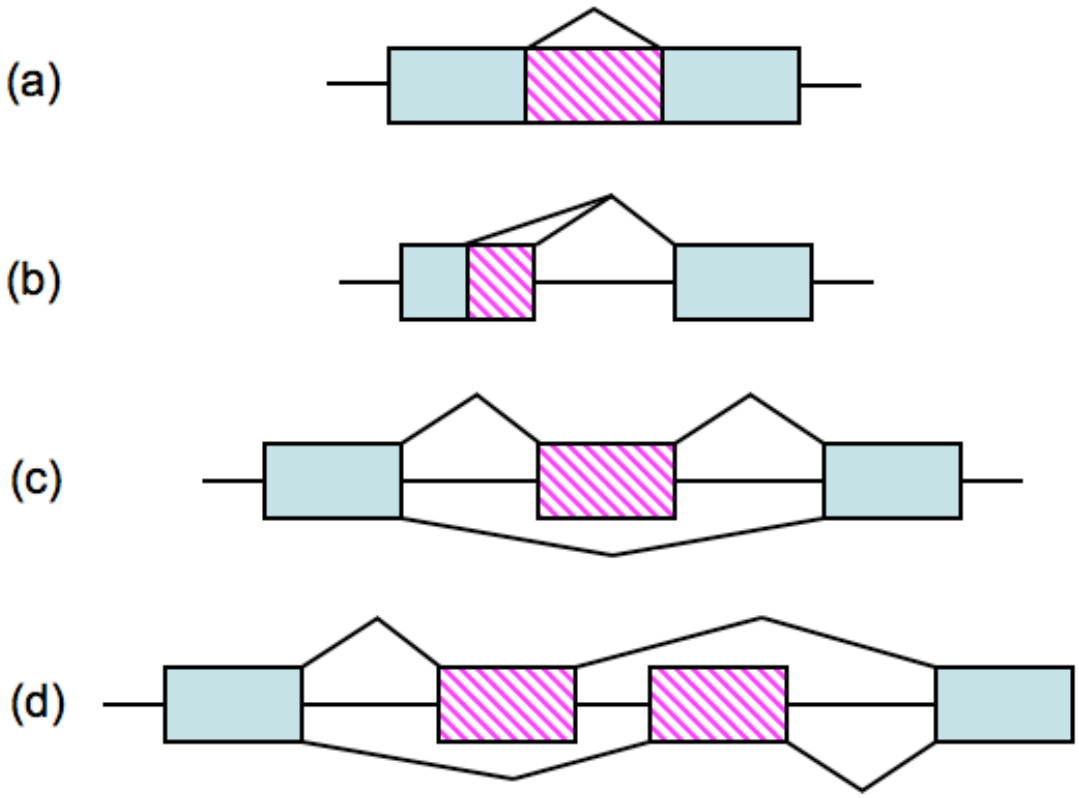

Figure 1. Different examples of alternative splicing.

(a) Retained intron, (b) competing 5'-splice sites (c) cassette exons, (d) mutually exclusive exons. Splicing patterns are illustrated by the diagonal black lines. Exons are denoted by the rectangles. Blue exons are constitutive; alternatively spliced segments are shown by the striped magenta boxes.

For TRPV1, there are currently 7 reported splice variants between humans, mice, and rats in the published literature for TRPV1 (Table 1). These variants are named TRPV1.b [70], TRPV1.β [71], TRPV1.var [78], TRPV1.5'sv [79], stretch-inactivated channel (SIC) [80], and two unnamed variants I have referred to as TRPV1.son [81] and TRPV1.ais [72]. TRPV1.son was identified in the supraoptic nucleus of mice. The SIC variant is controversial since it is allegedly a product of trans alternative splicing between TRPV1 (exons 6-14) and the C-terminal domain of TRPV4. It has not been independently confirmed [81,82]. Interestingly, 5 of the variants are generated from splicing events occurring in what will be the cytosolic N-terminal region of the mature protein, and all of them have splicing events occurring in the seventh exon, except TRPV1.var. TRPV1.β is both examples of alternate 3' splicing, utilizing cryptic splice sites to truncate exon 7 by 60 and 30 nucleotides, respectively. TRPV1.b is an example of a cassette exon, where the entire seventh exon is splice out. And TRPV1.var is an example of both an alternative transcriptional start site and a retained 110 base pair intron between exons 5 and 6. Though similar in splicing activity, these splice variants were isolated in three different organisms: human, rat, and mouse. The exact role and function of each of these splice variants is not settled, but the majority exert their effect by altering the channel's sensitivity [70] or act as dominant negative regulators [71,78].

Table 1. Known splice variants of TRPV1 and those discussed in this study

Name	Splicing Event	Original Species	Tissue Origin	Genbank Entry	Reference
TRPV1.var	Retained intron between exons 5 and 6	Rat	Kidney	N/A	Tian et al. (2006) [78]
TRPV1.SIC	Trans splicing of TRPV1 and TRPV4	Rat	Trigeminal and Dorsal Root Ganglia, Kidney	AB015231.3	Schumacher et al. (2000) [80]
TRPV1.5'sv	Translation begins at exon 5 and exon 7 is spliced out	Rat	Dorsal Root Ganglia	AF158248.2	Schumacher et al. (2000) [79]
TRPV1.b	Exon 7 is spliced out	Human	Human Brain	AY986821.1	Lu et al. (2005) [70]
TRPV1.β	Exon 7 is truncated by 30 bp	Mouse	Dorsal Root Ganglia	AY452084.1	Wang et al. (2004) [71]
TRPV1.ais	Unspecified	Rat Mouse	Tongue	N/A	Lyall et al. (2005) [72]
TRPV1.SON	Splicing in N-terminal region	Mouse	Brain	N/A	Sharif et al. (2006) [81]

While the role of these variants has been postulated under normal conditions, virtually no information is available about how these isoforms behave under different conditions, including neuropathic pain states. So far, only two paper have been published that attempt to describe how the expression of TRPV1.b is affected by different environmental factors [83,84]. Vos et al. (2006) showed that TRPV1.b results of the first paper showed that overexpression of TRPV1.b in HEK cells attenuates TRPV1's response to capsaicin, heat, and protons. Subsequently, Charrua et al. (2008) showed that TRPV1.b expression is downregulated in the DRGs of rats injected with cyclophosphamide, a compound that induces bladder inflammation and models the human disease cystitis.

Neuropeptide Y and Growth-associated Protein 43

In this study, the changes in expression of Neuropeptide Y (NPY) and Growth-associated Protein 43 (Gap43), in addition to the traditional behavioral tests normally conducted, serve as positive molecular controls for the Chronic Constriction Injury (CCI) model of neuropathic pain. NPY, like TRPV1, is another gene that is involved in the pain transduction pathway [85]. Unlike TRPV1, which forms ion channels located in nerve terminals and is a nocioceptor, NPY is a peptide neurotransmitter released by primary afferent neurons located in the Dorsal Root Ganglia and received by neurons located in the substantia gelatinosa region of the spinal cord [85]. In animal models of neuropathic pain, NPY has been shown to be massively upregulated [86,87]. It is believed that this increase in expression results in the decrease of action potentials in post-synaptic neurons by decreasing the influx of calcium ions, thereby decreasing the activation of Ca++ sensitive K+ channels [85,88]. The lowered activation of Ca++ sensitive K+ channels diminishes the intensity of the pain perceived by organism. The increase in NPY, therefore, is indicative that trauma to the nerve has occurred.

Gap43 is a growth-associated protein highly expressed in the growth cones of elongating axons. Its expression decreases after the target has been innervated [89]. In addition to its developmental role, Gap43 expression is differently expressed following neuronal tissue damage or inflammation, which has been demonstrated in many different animal neuropathy models [89,90,91]. Unlike NPY or TRPV1, Gap43 cannot be used to verify that a specific type of neuropathic pain state has been induced because it is not involved in the transduction of painful stimuli. However, it can be used to verify that trauma has been caused to peripheral nervous tissue.

Specific aims

This study began with two hypotheses. The first is that TRPV1 mRNA levels are altered in the dorsal root ganglia of Sprague Dawley rats following a peripheral nerve injury in a tissue-specific manner; the second is that mRNA levels of alternatively spliced isoforms of TRPV1 are also altered following a peripheral nerve injury. A third hypothesis was added midway through the study: that TRPV1 protein expression is increased in the dorsal root ganglia following a peripheral nerve injury.

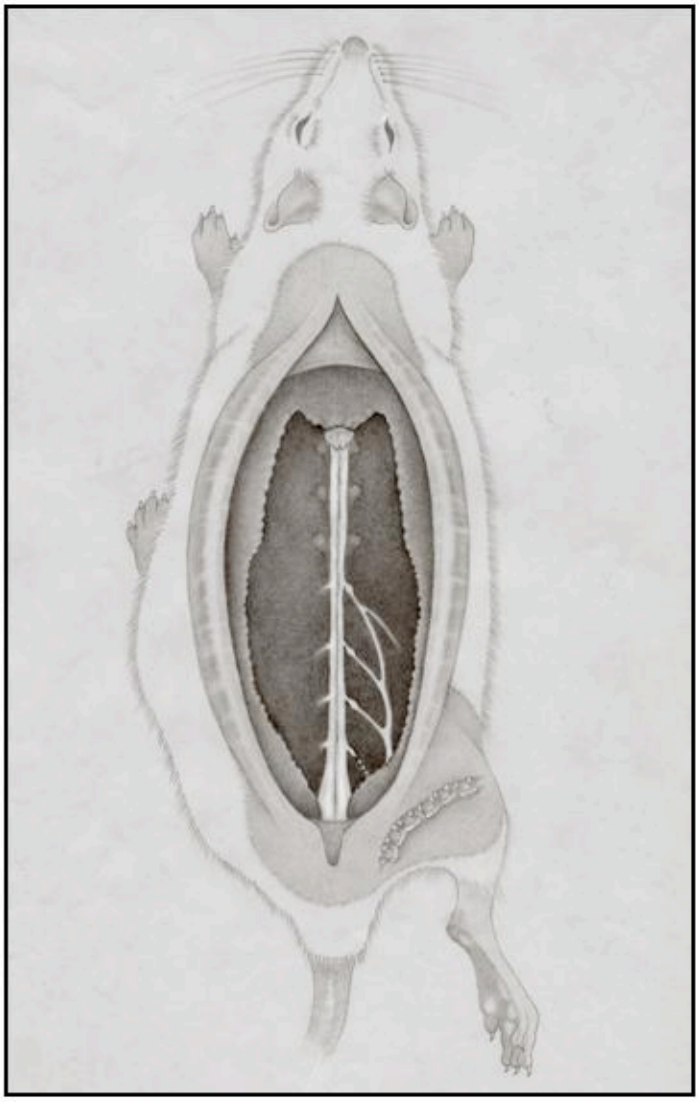

Figure 2. Dorsal view of Rat Neuroanatomy

From bottom to top are the L6, L5, L4, and L3 dorsal root ganglia projecting from the spinal cord. Attached to each of these dorsal root ganglia are the axons that give rise to spinal nerves. The spinal nerves combine to form the sciatic nerve mid-thigh. The axons from L4 and L5 constitute 98-99% of the total number of axons that comprise the sciatic nerve. L3 is suggested to contribute ~1.2% of total axons. The contribution to the sciatic nerve from L6 is variable and at most contributes 0.4% of the total axons. The autoclips shown mid-thigh are used to close the skin post-surgery (see methods).

Artwork kindly provided by Mr. Robert Hoggard.

CHAPTER 2

MATERIALS AND METHODS

Chronic constriction injury

This study was approved by the Institutional Animal Care and Usage Committee of Duquesne University. Twenty-two adult male Sprague-Dawley rats (Hilltop Lab Animals, Inc., Scottdale, PA, 212g) were used for the experiment.

The Chronic Constriction Injury (CCI) procedure, which was developed by Bennet and Xie [92] is used to simulate in rats the human neuropathic condition called Chronic Regional Pain Syndrome II (CPSII). CPSII is a disease that can occur after damage to a peripheral nerve, such as the sciatic nerve, has occurred. Symptoms of CPSII include spontaneous pain, hypersensitivity of the skin, mottling of the skin, and distal extremity swelling [93,94]. All training necessary for compliance with IACUC and the project was received from Dr. Somers, a professor of the Physical Therapy department at Duquesne University. He is an expert at performing this surgery and has used it extensively in his own research [94,95,96]. Rats undergoing CCI were anesthetized with sodium pentobarbital (50 mg/kg) via intraperitoneal injections. To confirm that the rats were sufficiently anesthetized, the tail-pinch and leg withdrawal tests were performed. Prior to surgery, the entire right leg and a portion of the lower back is shaved with an electric razor. The surgical site, the rear right thigh, was depilated

with Nair, a commercial hair-removal product. Betadine, a povidone-iodine solution, was applied to leg to help prevent infections from occurring. The surgeries began with an incision in the mid-thigh region. The sciatic nerve was exposed by separating the Gluteus superficialis and biceps femoris muscles. To liberate the sciatic nerve, the fascia that keeps it attached to the biceps femoris was cut. Once free, four 4.0 chromic gut sutures were loosely tied around the sciatic nerve in 1mm intervals. Care was taken to prevent the sutures from being overly tight, such that blood flow through the epineurial vasculature was not stopped. During the procedure, animals were administered additional small doses of anesthetic (~6mg/kg) to maintain the correct amount of anesthesia during the procedure. The wound was closed in layers, using 4.0 silk sutures to sew the muscles back together and autoclips to close the skin. See Figure 3 for details and photographs of the procedure. Two other groups of animals were used in this study: control and sham animals. Sham animals underwent the surgery as described above, but sutures were not tied around the sciatic nerve. The control animals were not operated on, nor did they receive any anesthetic.

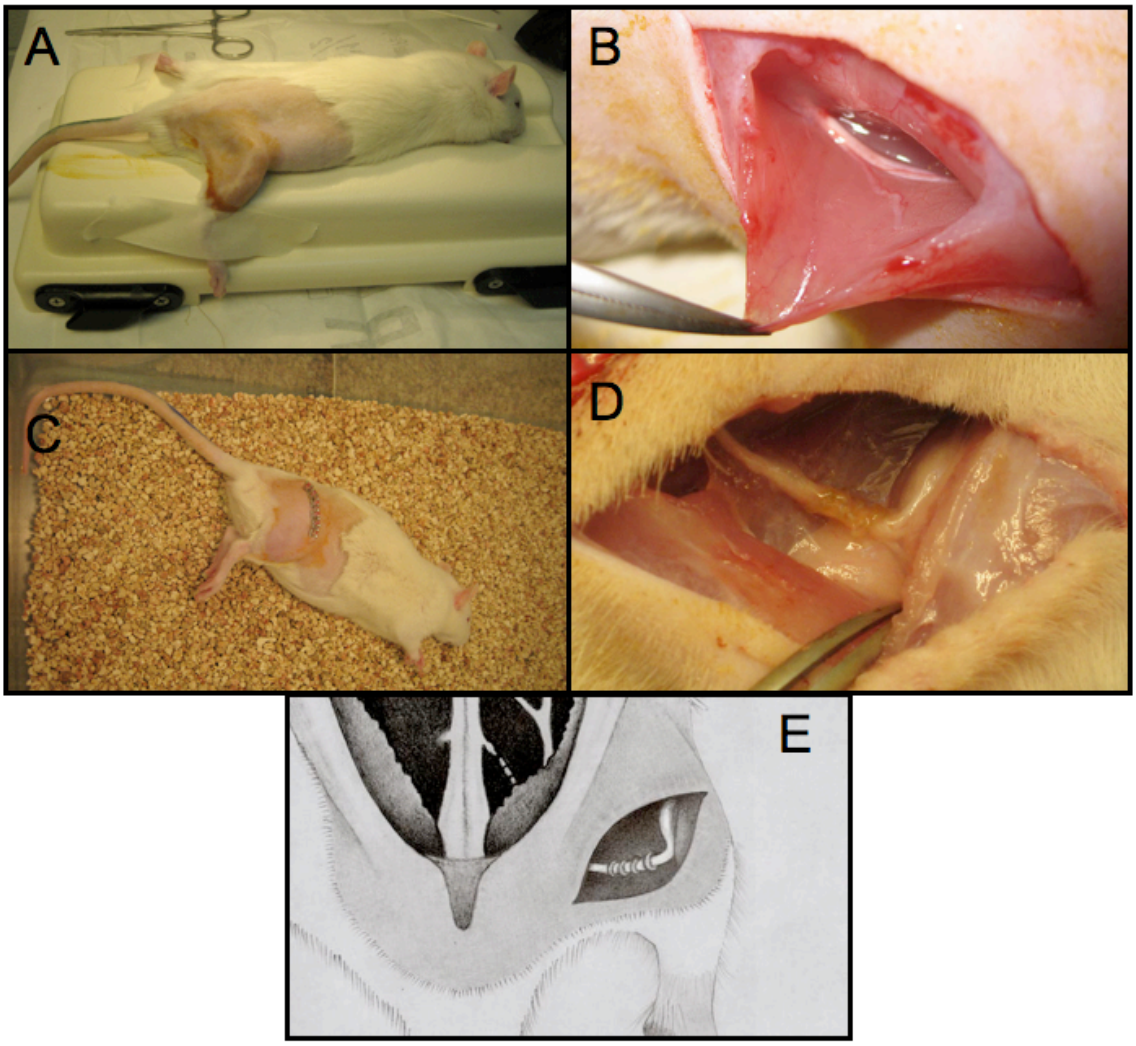

Figure 3. Chronic Constriction Injury Surgery

(A)Pre-surgery. The rat is anesthetized with pentobarbital. Then its rear leg is shaved, depiliated, and treated with betadine to sterilize the surgical site.
(B) Surgery. An incision is made to separate the gluteus superficialis from the biceps femoris, exposing the sciatic nerve. The forceps are shown pulling the biceps femoris away from the gluteus superficialis, exposing the sciatic nerve.
(C) Post-surgery. The muscles are sewn back together and the skin is closed with autoclips. The still anesthetized rat is then returned to its cage.
(D) Ligated sciatic nerve. Four 4.0 sutures are tied around the sciatic nerve. The lack of perfusion is a result of the photograph being taken post-mortem.
(E) Sketch of the sciatic nerve with sutures in place. The spinal cord and the combined L4 and L5 spinal nerves are shown. These two spinal nerves form the bulk of the sciatic nerve.

Photograph (D) kindly provided by Bree Zeyzus Johns
Artwork (E) kindly provided by Mr. Robert Hoggard.

Behavioral assessment

Two behavioral tests were performed on day 0, the day on which the CCI and sham animals underwent surgery, and again on days 8 and 11 post-operation. Baseline behavioral assessments were performed prior to any operation. These tests were used to determine if mechanical allodynia (pain felt from stimuli that normally do not cause pain) or thermal hyperalgesia (an increased pain sensation) had been induced; both symptoms are common characteristics of neuropathic pain caused by the CCI procedure. A timeline for the assessment procedure can be seen below:

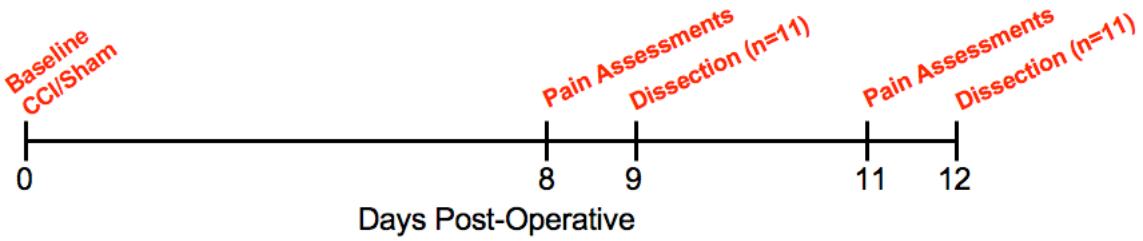

Figure 4. Experimental Timeline for Animal Work

Mechanical and thermal baseline pain assessments were conducted for the three treatment groups at day 0 prior to any surgical procedures. Pain assessments were repeated at days 9 and 11 post-operation. 11 animals (3 control, 4 sham-treatment, and 4 CCI-treatment) were sacrificed on days 9 and 11. DRGs were dissected out and stored for further use.

On each day of testing, mechanical allodynia tests were performed first. Testing for mechanical allodynia was performed by using calibrated Semmes-Weinsten monofilaments. To ensure that any response would be correlated with the ligation of the sciatic nerve, the monofilaments were only applied to plantar surface of the rats' right rear paw, which is an area only innervated by that nerve. The rats were placed in

plexiglass boxes with exposed wire bottoms. They were then allowed to habituate to this environment for 5 minutes. Then, the filaments were applied to one paw at a time in order of thickness, from thinnest to thickest (0.41, 1.2, 3.63, 8.51, 15.13g). The number of withdrawals per paw was recorded for each filament. To prevent stimulation fatigue, each paw only received 5 pokes from one filament in one trial, and a total of two trials were performed per filament. One trial consisted of each paw being poked 5 times. Each trial was separated by five minutes. The testing was complete when an animal was poked with all filaments or when a rat withdrew from all 10 pushes for a single filament.

To determine the 50% withdrawal threshold for each rat, a linear regression method was used. The 50% withdrawal threshold is the calculated force (g) at which a rat will withdraw its paw 5 out of 10 pokes from one filament. If the calculated value exceeds 15.13g, the force to deflect the thickest filament, then that value was recorded as the 50% withdrawal value. The formula for determining the 50% withdrawal value can be calculated using the formula below:

Normalized 50% withdrawal threshold (WT) = Post-Surgery (50% WT right paw — 50% WT left paw) – Baseline (50% WT right paw – 50% WT left paw).

For each treatment group, all normalized withdrawal latencies were averaged, and the mean values were compared using the Kruskal-Wallis 1-Way ANOVA by Ranks Test. This was done for day 8 and day 11.

Following the mechanical sensitivity tests, I allowed the rats to rest in their home cages for 5 minutes before performing the thermal sensitivity test, which measured thermal hyperalgesia. Each rat was placed inside of a plexiglass chamber on top of the radiant heat source and allowed to habituate to the chamber for 5 minutes. After the habituation period was completed, the glass beneath the plantar portion of each rear paw was heated, though only one paw was irradiated at a time. The rats were allowed 5

minutes of rest between irradiation treatments. The source of heat for this apparatus came from a slide projector bulb that is focused through a fixed diameter aperture. The irradiation began when an operator-controlled switch was thrown, and stopped either when the rat raised its paw, which interrupted a photocell that receives reflected light off of the paw, or when the irradiation had occurred for the maximum period of 20 seconds. Each paw received five treatments, which were averaged to produce a mean withdrawal latency. Withdrawal latencies were measured in hundredths of a second. The formula used to calculate each rat's normalized withdrawal latency is as follows:

Normalized Withdrawal (WD) Latency = Post-Surgery (WD latency right paw – WD latency left paw) – Baseline (WD latency right paw – WD latency left paw).

For each treatment group, all normalized withdrawal latencies were averaged, and the mean values were compared using the Kruskal-Wallis 1-Way ANOVA by Ranks Test. This was done for day 8 and day 11. The normalization process accounts for changes in behavior over a period of time, and any differences in response between a rat's contralateral and ipsilateral paws. See Figure 5 for details.

Nocifensor signs of behavior were observed during the course of testing, but no systematic record of their occurrence was kept. The types of behavior that were observed included paw-licking, paw-waving, paw-guarding, and defensive posturing. Paw-licking and paw waving would occur rapidly after a paw had been poked or irradiated. Paw-guarding is defined as the prolonged raising of the affected paw off the ground. Its occurrence was noted more often during the middle of a testing period and between rounds of testing. Defensive posturing would occur when a rat would not stand with all four paws on the ground, and instead would either lie on its side or stand on its two rear feet, preventing me from testing it.

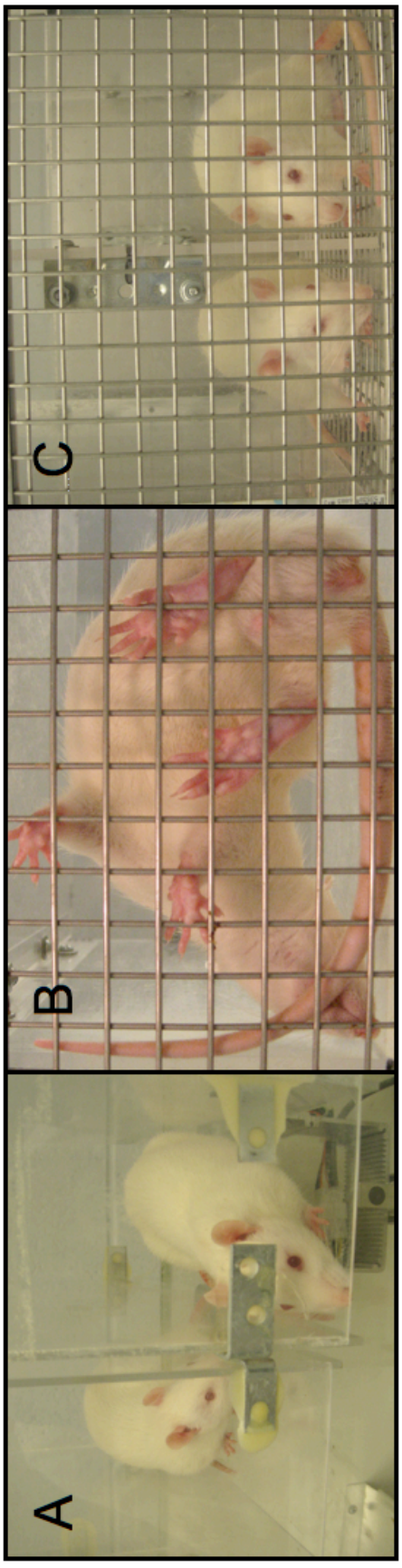
C
B
A

Figure 5. Behavioral Testing Setup

(A) Thermal pain assessment. Rats were placed inside plexiglass boxes on top of the testing apparatus. Thermal hyperalgesia was tested by focusing a radiant heat source onto the glass beneath their rear paws. Withdrawal was recorded in milliseconds.
(B) Plantar portion of the rear paws. The arrowheads are pointed at the plantar portion of the rear paws, which is between the the heel and the pads at the front of the paws.
(C) Mechanical pain assessment. Rats were placed inside of plexiglass boxes atop of a wire grid. Mechanical allodynia was tested by poking the plantar portion of the rats' hind paws with calibrated monofilaments.

Dorsal root ganglia removal

At days 9 and 12 post-operation, the ipsilateral and contralateral dorsal root ganglia (DRG) from lumbar levels 2-6 were removed. On each day, 3 control, 4 CCI, and 4 Sham animals were sacrificed (n = 11 per collection day). First, the animals were anesthetized with sodium pentobarbital (50mg/kg) intraperitonealy. The tail-pinch and leg withdrawal tests were again employed to ensure deep anesthetization. Then an incision was made along the length of the spine, exposing the muscles and spine. The muscles attached to spine were removed, exposing the spinous and lateral processes of the lumbar vertebrae. With medical rongeurs, the spinous processes were removed. The dorsal lumbar vertebrae were then shaved down using a Dremel drill. The remaining bone was removed with Rongeurs and forceps, exposing the spinal cord and DRGs. The DRGs were removed with forceps and microscissors. Once extracted, the DRGs were immediately submerged in *RNAlater* (Qiagen), a solution designed to stabilize RNA, and placed on ice until they could be transferred to the -80C freezer. After all of the DRGs were removed, the rats were sacrificed via thoracotomy. See Figure 2 for an illustration of rat neural anatomy and Figure 6 for photographs of the procedure.

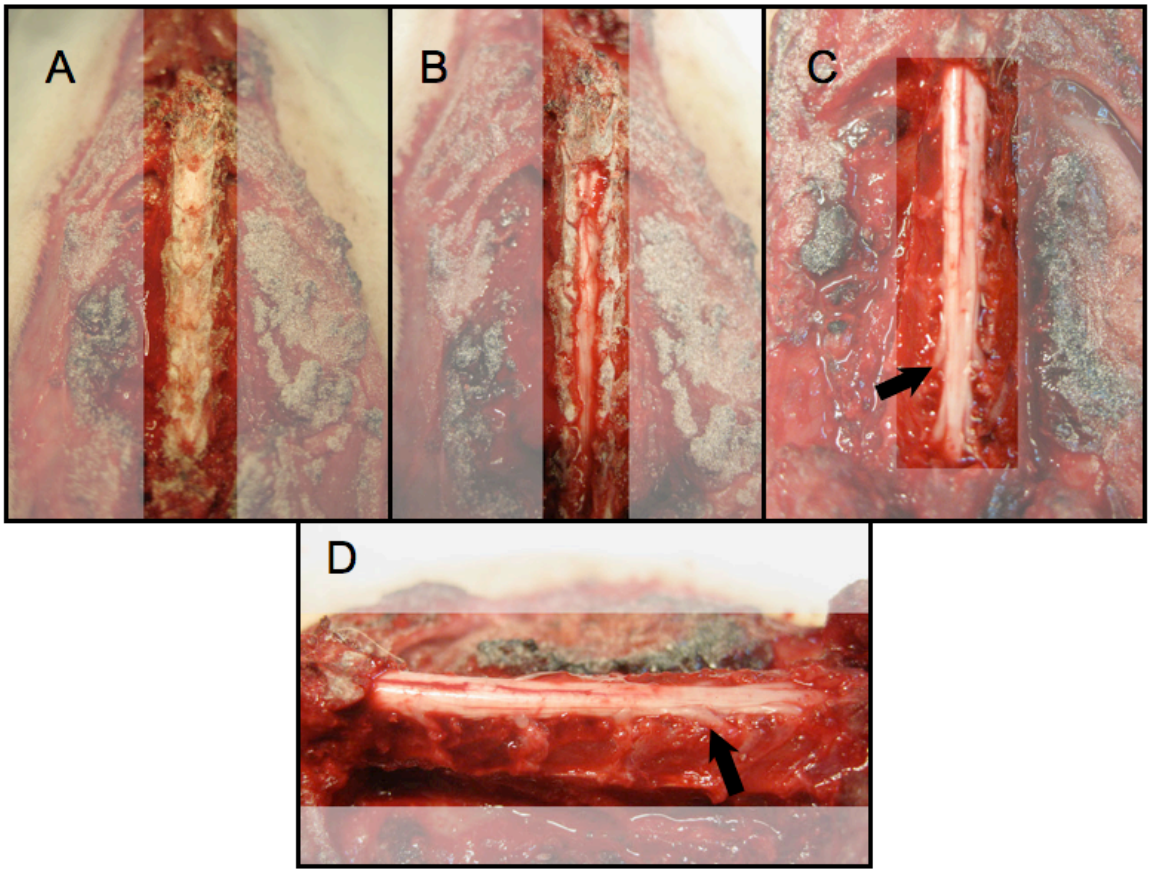

Figure 6. Dorsal Root Ganglia Removal

(A) The skin and muscle are removed to expose vertebrae. Spinal processes are removed and the bone is shaved down.
(B) Bone is removed with forceps and rongeurs to expose the spinal cord.
(C) The remaining bone has been removed, revealing underlying spinal column and dorsal root ganglia (L2-L6 exposed). Arrow points to left L5 DRG.
(D) Lateral view of exposed spinal column and dorsal root ganglia (L2-L6 exposed). The Arrow points to left L5 DRG.

RNA isolation and cDNA generation.

Tissue samples were removed from the RNAlater solution, cut into small fragments, placed into a lysis buffer, and then run over QiaShredder columns to ensure complete homogenization. Total RNA was then extracted using the RNeasy kit (Qiagen). To prevent any genomic DNA contamination, each RNA sample was treated with DNase I (Invitrogen). Complementary DNA (cDNA) was generated using poly-dT primers during the reverse-transcription reaction (Superscript III, Invitrogen). Poly-dT primers only target mRNA transcripts by annealing to their polyA tails. 2μL of RNA was used in each reaction. For each tissue sample, two 100μL pools of cDNA were generated by combining five 20μL reactions. The 5 reactions were combined because Zeyzus [66] found that each reaction would produce a variable concentration of cDNA, and combining them would produce a uniform cDNA concentration. cDNA samples were stored at -20C until used. Each 100μL pool of cDNA was tested separately.

cDNA analysis and RNA quantification

RNA was quantified using two similar techniques, often referred to as 1-step and 2-step quantitative PCR (qPCR). 2-step qPCR was performed using cDNA prepared in the manner described previously, and 1-step qPCR was performed using RNA as the template. The difference between 1-step qPCR and 2-step qPCR is that for 1-step reactions the reverse-transcription and amplification occur in the same test tube, and gene specific primers are used instead of poly-dT primers during the reverse-transcription.

Samples were analyzed in triplicate, and at least twice. Prior to being used for qPCR, all primer sets were tested with conventional PCR. See Table 2 for primer information

Table 2. Primer sequences used for this study.

GAPDH				
	Tm (°C)	GC content (%)	Sequence (5'-3')	Amplicon length
Forward	55.4	55.0	CACAGTCAAGGCTGAGAATGG	
Reverse	54.7	55.0	CGATGCCAAAGTTGTCATGG	
				300bp
TRPV1				
	Tm (°C)	GC content (%)	Sequence	Amplicon length
*Forward	56.2	55.0	GTGATCGCTTACAGCAGCAG	
*Reverse	55.0	55.0	CGGTGACTCGGAAATAGTCC	
				238bp
TRPV1.b				
	Tm (°C)	GC content (%)	Sequence	Amplicon length
*Forward	51.2	42.9	TACACAGACAGCTACTACAAG	
*Reverse	53.4	50.0	ATGACGGTTCCCGATCTT	
				471bp
TRPV1.β				
	Tm (°C)	GC content (%)	Sequence	Amplicon length
Forward	51.7	50.0	GTTCTGGAGAACCGTCAT	
Reverse	51.6	45.0	CACAAACAAACTCTTGAGGG	
				312bp
TRPV1.var				
	Tm (°C)	GC content (%)	Sequence	Amplicon length
Forward	55.7	55.0	ATCATCCAGGGACTAGCCTC	
Reverse	56.8	52.3	CAGCAGGAACTTCACAATGGC	
				121bp
TRPV1.E7				
	Tm (°C)	GC content (%)	Sequence	Amplicon length
Forward	59.3	61.1	AACTCCACCCCACGCTGA	
Reverse	57.6	57.8	CGGTTCAAGGGTTCCACGA	
				307
NPY				
	Tm (°C)	GC content (%)	Sequence	Amplicon length
Forward	49.6	47.4	GACAGAGATATGGCAAGAG	
Reverse	48.9	47.4	CTAGGAAAAGTCAGGAGAG	
				148bp
Gap43				
	Tm (°C)	GC content (%)	Sequence	Amplicon length
Forward	51.0	50.0	CCTAAACAAGCCGATGTG	
Reverse	49.7	44.0	TTTGGCTTCATCTACAGC	
				150bp

* = primer sequences acquired from Charrua et al. (2007).

Two different qPCR machines were used during this study—a StepOnePlus 96-well real-time machine from Applied Biosystems, and a Rotor-Gene Q from Qiagen. For all 2-step reactions performed on the Rotor-Gene Q, Express SYBR GreenER master mix (Invitrogen) was used. The following reaction conditions were used: 50°C UDG incubation (2'). 95°C Hot start (2') [95°C (20"), 60°C (30"), 65°C (60")]$_{40}$. For all 2-step reactions performed on the StepOnePlus, Power SYBR Green master mix (Applied Biosystems) was used. The following reaction conditions was used: 95°C (10') [95°C (15"), 60°C (60")]$_{45}$. All 1-step reactions were performed on the StepOnePlus machine using the *Power* SYBR® Green RNA-to-C_T™ *1-Step* Kit (Applied Biosystems). Reaction conditions for 1-Step reactions were as follows: 48°C Reverse Transcription (30'), 95°C AmpliTaq activation (10'), [95°C (15"), 60°C (60")]$_{40}$. Samples were prepared in 0.2mL PCR tubes or 48 well plates, and all final reaction volumes were 20μL.

For all reactions performed on the Qiagen machine, the "Noise Slope Correct" analysis setting was applied in order to minimize background fluorescence. No equivalent setting was available for the StepOnePlus machine. However, a threshold value of 0.1 was selected for all reactions using the StepOnePlus machine. A melt curve analysis was performed after each reaction to ensure that a single product was being amplified and to help minimize the occurrence of primer-dimer.

Visual analysis of amplified cDNA products were analyzed via an ethidium bromide stained agarose gel. All gels were 2.5% and run in 1x TAE buffer for 100 minutes at 100 volts.

Subcloning and sequencing

cDNA clones for TRPV1.b, TRPV1.can, TRPV1.β, and TRPV1.E7 were generated using the TOPO TA cloning kit (Invitrogen). cDNA samples were generated by conventional PCR, using the primers listed above. Single product formation was verified by gel electrophoresis. Following PCR, the samples were purified using the Minelute PCR Purification Kit (Qiagen), either directly from PCR product or isolated from a gel. The cDNA samples were ligated into the pCR®2.1-TOPO® Vector, which was then transformed into Mach1^{TM}-T1^{R} chemically competent cells.

Plasmids were harvested using the Purelink^{TM} Quick Plasmid Miniprep kit (Invitrogen). They were screened for successful insertion with PCR, using M13 primers, and gel electrophoresis. Plasmids carrying inserts were sequenced using the BigDye® Terminator Sequencing kit using both the forward and reverse M13 primers (Applied Biosystems). They were then entered into the BLAST algorithm for confirmation. Confirmed sequences were then entered into the ClustalW alignment program alongside predicted DNA sequences, which were generated by me ahead of time. Sequence data for TRPV1.E7 and TRPV1.can were kindly provided by Metis Hasipek and Karina Pena, respectively.

Immunohistochemistry and confocal microscopy

DRGs from two rats, one control and one CCI, were used for fluorescent microscopy. The CCI rat underwent the same surgery as described above. However, prior to the surgery, the plantar region of the rat's right rear paw was injected with DiD Dye (Molecular Probes), which is a retrograde tracer and will stain all DRG neuronal

cells that innervate the region. The control rat was also injected with the retrograde dye also under anesthesia (50mg/kg). Twelve days post-treatment, all DRGs from lumbar levels 2-6 were removed and immediately submerged in a 4% paraformaldehyde 1X phosphate buffer saline (PBS). They were stored at 4°C until processed.

To cryoprotect the tissue samples, they were placed in a 30% sucrose 1X PBS solution for 4 hours. Approximately 1/3 of the solution was then removed and replaced with Optimal Cutting Temperature (OCT) compound (Sakura) and incubated on a rocking shaker overnight. The samples were then mounted in OCT and cut into 20μM slices on a cryostat. Care was taken to orient the DRGs in the OCT so that samples were cut starting with the end distal to the spine to the proximal end. Slices were thaw-mounted onto critically-cleaned slides and post-fixed in a 4% paraformaldehyde 1X PBS solution. The slides were then washed twice in 1X PBS and stored in 1X PBS until stained. Prior to staining, the slices were permeabilized in a 0.3% Triton-X 100 1X PBS solution, and then washed twice more in 1X PBS. The tissue samples were treated with 20μL of the primary antibodies and incubated overnight at 4°C. The following primary antibodies were used: 1:50 mouse anti-rat Neurofilament (Neuromics), 1:50 rabbit anti-rat TRPV1 (Santa Cruz Biotechnology). The sections were then washed three times in PBS and incubated overnight with secondary antibodies conjugated to Alexa-546 (Molecular Probes), or FITC (Santa Cruz Biotechnology), and diluted 1:100 in PBS. Sections were washed in 1X PBS and mounted in Prolong-Gold (Invitrogen). Fifteen Superlab III students participated in the staining and imaging of the tissue sections under the guidance of myself and Dr. John Pollock.

Fluorescent images were collected by Dr. John Pollock using a Leica TCS SP spectral confocal microscope, which facilitates acquisition of multicolor images. Relative expression of TRPV1 was determined by comparing it to expression of DiD, whose expression is not affected by the CCI surgery. This was done for neurons from control DRGs and CCI DRGs. The relative expression of TRPV1 from each tissue sample and the difference between the two was recorded.

Statistical analysis

The α level was 0.05 for all statistics. All statistical tests were performed using SPSS software, version 18 for the Windows operating system (SPSS Inc., Chicago, IL). One-way ANOVA tests were performed to determine statistical significance of the quantitative real-time PCR studies. Kruskal-Wallis One-way ANOVA by Ranks tests were performed to determine the statistical significance of the mechanical and thermal behavioral data. Assistance with statistical analysis was kindly provided by Dr. Sarah Woodley and Dr. Dave Somers.

Chapter 3

RESULTS

Chronic constriction injury surgery causes pain

Visual observations of the rats' behavior suggested that the CCI surgery had induced a chronic pain state in the affected animals. During both tests, the rats would display nocifensorous behaviors, such as paw-licking, paw-waving, paw-guarding and defensive posturing. The behaviors were also observed to be more severe at day 11 than at day 8. The rats were also observed limping in their cages, favoring the affected paw, and minimizing the amount of weight it supported. However, these visual observations were not substantiated by the results of the thermal and mechanical behavioral testing.

Thermal hyperalgesia

One of the most common symptoms of CCI-induced neuropathic pain in rats is thermal hyperalgesia, which is an elevated response to a non-painful or mildly painful heat source. Thermal hyperalgesia was assessed by comparing the normalized mean withdrawal latencies (pain scores) from a radiant heat source of the CCI-treatment, sham-treatment, and control groups. At day 8 post-surgery, the mean withdrawal latency for the CCI-treatment, sham-treatment, and control groups were -0.31±1.87, 2.11±0.74, and 2.11±0.86, respectively (Figure 7). The CCI-treatment group was not significantly different from the sham-treatment or control group Nor was the sham-treatment group

different from the control group. At day 11 post-surgery, the mean withdrawal latency for the CCI-treatment group, sham-treatment group, and control group were -1.16±0.65, 0.41±1.54, and -0.74±2.67, respectively. Though lower than either the control or sham-treatment group, the CCI-treatment group was not significantly different from either. The sham-treatment group was also not significantly different from the control group. These data cannot be used as evidence that the CCI procedure caused a greater amount of thermal hyperalgesia than the sham surgery, or that the procedure caused thermal hyperalgesia at all. See Figure 7.

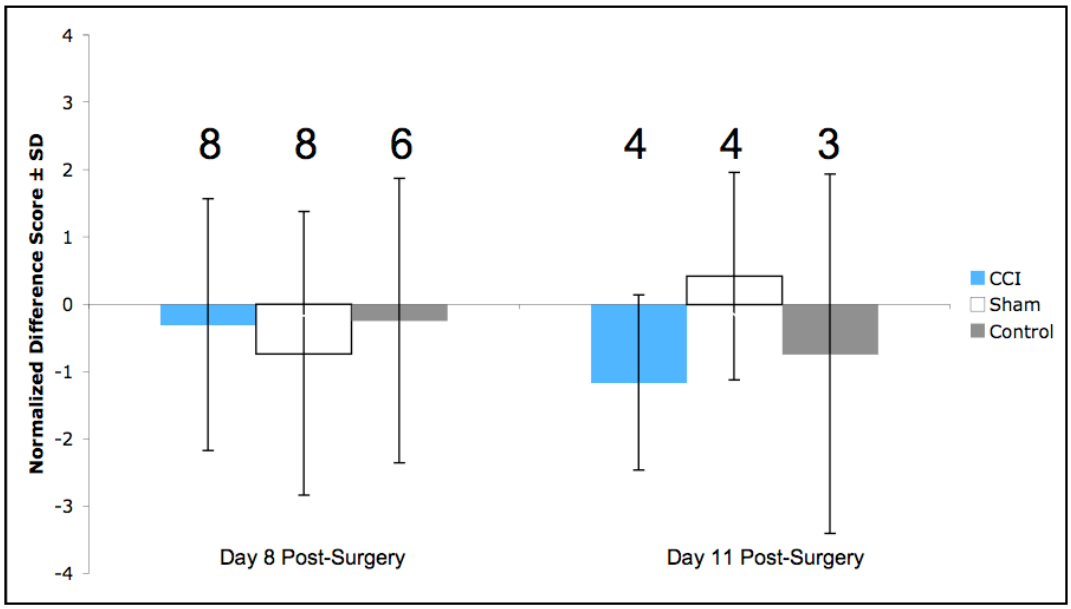

Figure 7. Thermal hyperalgesia in the right rear paw.

Bars represent the mean ± standard deviation (SD) normalized withdrawal latency from a radiant heat source for each treatment group at day 8 and 11 post-surgery. Lower threshold values indicate that the animals were experiencing an increased amount of thermal hyperalgesia. No significant differences were found between any treatment groups at either time point. The sample sizes for each treatment group at either time point are shown above the bars.

Mechanical allodynia

The other common symptom of CCI-induced neuropathic pain in rats is mechanical allodynia. Allodynia occurs when a normally non-painful stimuli is able to evoke a pain response. The 50% withdrawal method, as described previously, was used to calculate the normalized mean threshold for the three treatment groups at days 8 and 11. At day 8, the mean normalized 50% withdrawal threshold for the CCI-treatment sham-treatment, and control rats were, -0.73±1.54, 0.00±0.00, and 0.00, respectively (Figure 8). The CCI-treatment group was not significantly different from the sham-treatment or control group At day 11, the mean normalized 50% withdrawal threshold for the CCI-treatment, sham-treatment, and control rats were -2.46±2.88, 0.00±0.00, 0.00, respectively. The CCI-treatment group had a normalized mean withdrawal threshold lower than either the control rats or sham surgery rats, but was not statistically significant. The fact that the CCI-treated animals did not have more negative scores at day 11 is due to only 2 of the 4 animals having lowered threshold values. The other two animals showed no change in response to the mechanical stimuli.

At day 8, the mean normalized 50% withdrawal threshold for the sham-treatment group was not significantly different than the control group. At day 11, the mean normalized 50% withdrawal threshold for the sham-treatment group was not significantly different from the control group. Though the CCI-treatment group did have a lowered mean threshold value from the control group, it was not as great of a difference as has been recorded in previous studies by Zeyzus [66] or Somers [95]. For comparison, the

CCI-treatment rats from the study by Zeyzus had a normalized withdrawal mean of -5.0±3.98 day 11 post-surgery.

Fewer nocifensive behaviors were observed during the mechanical testing. The most common behaviors seen were weight shifting, to reduce the amount of support the affected paw had to contribute, and paw curling, which reduced contact between the plantar surface with the wire-bottom. These behaviors were also not recorded.

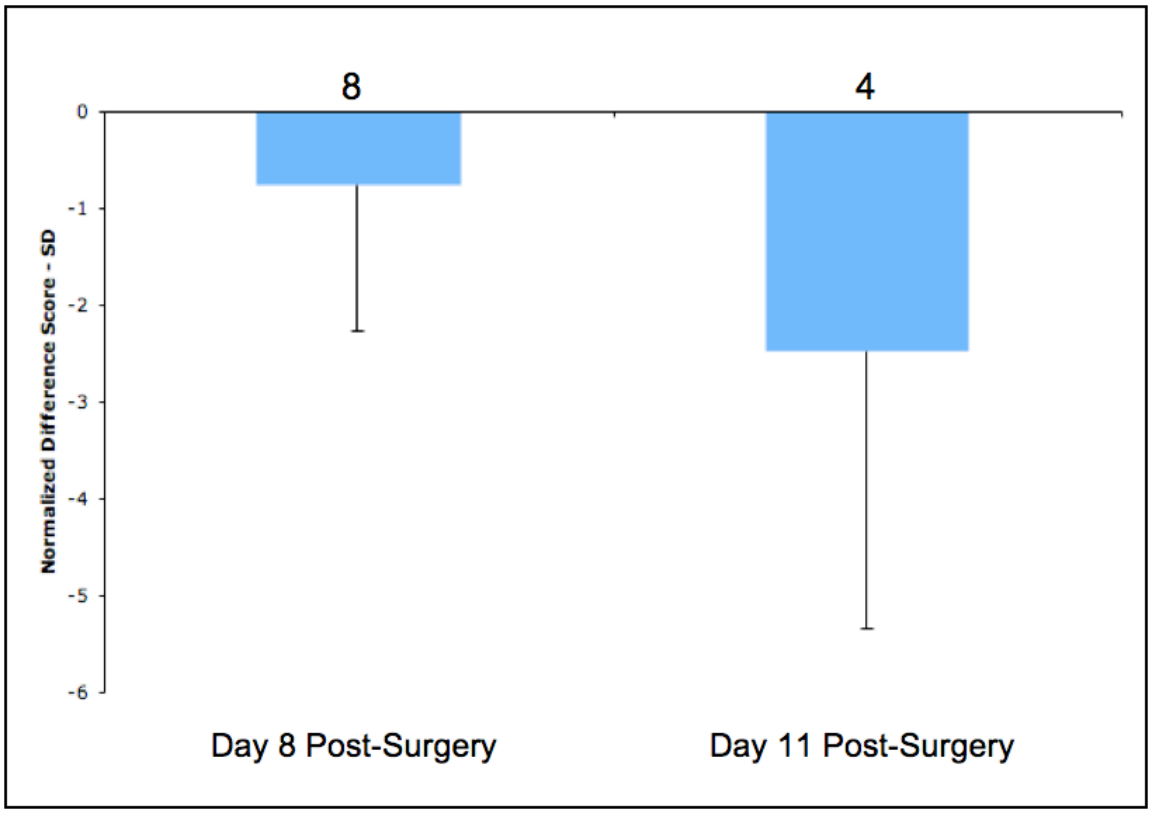

Figure 8. Mechanical allodynia in the right rear paw.

Bars represent the mean normalized 50% withdrawal threshold from calibrated Semmes-Weinstein monofilaments (g) for only the chronic constriction injury treatment group. Error bars represent standard deviation. No changes in withdrawal thresholds were recorded for the sham-treatment group or control group, and are not shown here. Lower scores indicate that the animals' threshold for mechanical stimuli have been lowered. There is no significant difference between the control group and the CCI-treatment group at either time point. Sample size for the CCI-treatment group is shown above each bar.

Sequence data: TRPV1 and splice variants are expressed in DRG

Sequence data confirmed that the primers for TRPV1, TRPV1.b, TRPV1.β, were amplifying the correct gene or splice variant. Gels for TRPV1 and the splice variants can be seen in Figure 9. ClustalW results for TRPV1.can, TRPV1.b, and TRPV1.β can be seen in Figures 10-12. In the figures, the sequenced data are compared to published sequences in Genbank. Since the variant specific primers were developed to span a spliced out region of the cDNA, the inclusion of the entire sequence corresponding to the location of primer site can be taken as confirmation of the existence of the variant. The confirmation of these sequences guaranteed that all subsequent reactions were done in full confidence that the right product was being analyzed. This is the first time that TRPV1.β has been isolated in rat DRG since it has only been previously documented in mice DRGs [71].

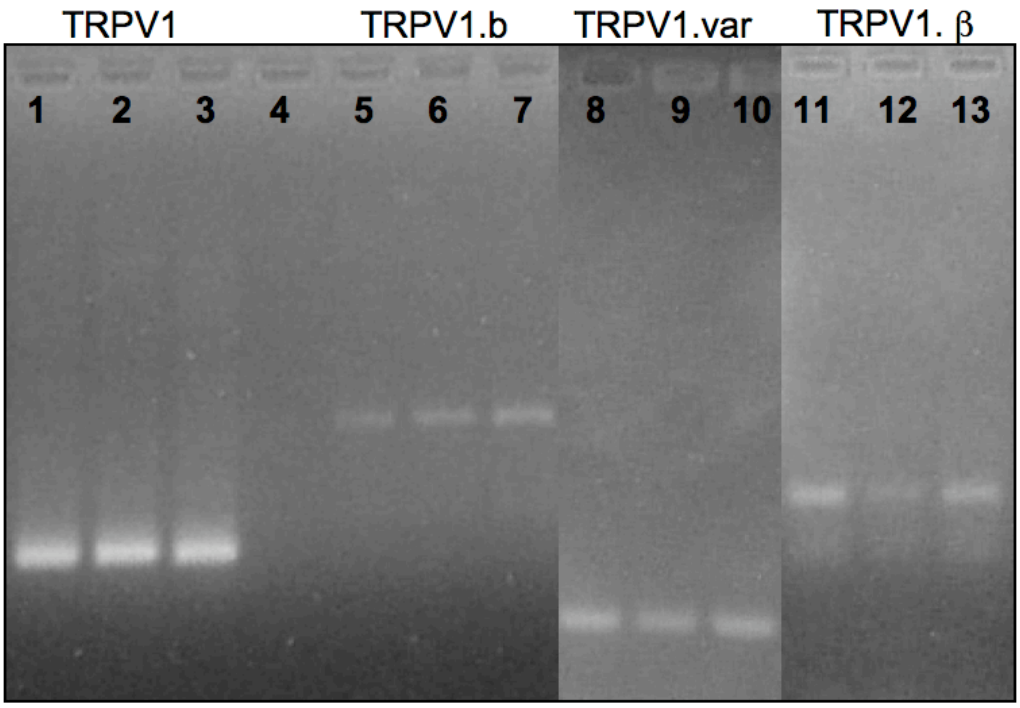

Figure 9. Gel visualization of TRPV1 and its splice variants following qPCR

Lanes 1-3 show the relative intensity of TRPV1 (238bp). Lanes 5-7 show the relative intensity of TRPV1.b (471bp). Lanes 8-10 show the relative intensity of TRPV1.var (121bp). Lanes 11-13 show the relative intensity of TRPV1.β (312bp). The image was assembled from three separate gels.

```
SeqA Name      Len(nt)  SeqB Name      Len(nt)  Score
=================================================
1    colony7   300      2    v1can     238      100
=================================================

colony7         GTAACGGCCGCCAGTGTGCTGGAATTCGCCCTTGTGATCGCTTACAGCAGCAGTGAGACC 60
v1can           ---------------------------------GTGATCGCTTACAGCAGCAGTGAGACC 27
                                                  *************************

colony7         CCTAACCGTCATGACATGCTTCTCGTGGAACCCTTGAACCGACTCCTACAGGACAAGTGG 120
v1can           CCTAACCGTCATGACATGCTTCTCGTGGAACCCTTGAACCGACTCCTACAGGACAAGTGG 87
                ************************************************************

colony7         GACAGATTTGTCAAGCGCATCTTCTACTTCAACTTCTTCGTCTACTGCTTGTATATGATC 180
v1can           GACAGATTTGTCAAGCGCATCTTCTACTTCAACTTCTTCGTCTACTGCTTGTATATGATC 147
                ************************************************************

colony7         ATCTTCACCGCGGCTGCCTACTATCGGCCTGTGGAAGGCTTGCCCCCCTATAAGCTGAAA 240
v1can           ATCTTCACCGCGGCTGCCTACTATCGGCCTGTGGAAGGCTTGCCCCCCTATAAGCTGAAA 207
                ************************************************************

colony7         AACACCGTTGGGGACTATTTCCGAGTCACCGAAGGGCGAATTCTGCAGATATCCATCACA 300
v1can           AACACCGTTGGGGACTATTTCCGAGTCACCG----------------------------- 238
                ******************************
```

Figure 10. Sequence Data for TRPV1

Sequence data was generated using the Big Dye Terminator kit from Applied Biosystems. Cloned Sequences were compared to Genbank entries using the ClustalW program. The 100% alignment score between the clone and the Genbank entry shows that the primers in these reactions successfully targeted TRPV1.

```
SeqA Name      Len(nt)  SeqB Name      Len(nt)  Score
=====================================================
1    colony4   522      2    TRPV1b    471      99
=====================================================

colony4          GAGGATGCTCGAGCGGCCCAGTGTGATGGATATCTGCAGAATTCGCCCTTTACACAGACA 60
TRPV1b           ------------------------------------------------------TACACAGACA 10
                                                                       **********

colony4          GCTACTACAAGGCCCAGACAGCACTGCACATTGCCATTGAACGGCGGAACATGACGCTGG 120
TRPV1b           GCTACTACAAGGGCCAGACAGCACTGCACATTGCCATTGAACGGCGGAACATGACGCTGG 70
                 ************ ********************************************

colony4          TGACCCTCTTAGTGGAGAATGGAGCAGATGTCCAGGCTGCGGCTAACGGGGACTTCTTCA 180
TRPV1b           TGACCCTCTTGGTGGAGAATGGAGCAGATGTCCAGGCTGCGGCTAACGGGGACTTCTTCA 130
                 ********** ********************************************

colony4          AGAAAACCAAAGGGAGGCCTGGCTTCTACTTTGGTGAGCTGCCCCTGTCCCTGGCTGCGT 240
TRPV1b           AGAAAACCAAAGGGAGGCCTGGCTTCTACTTTGGTGAGCTGCCCCTGTCCCTGGCTGCGT 190
                 ************************************************************

colony4          GCACCAACCAGCTGGCCATTGTGAAGTTCCTGCTGCAGAACTCCTGGCAGCCTGCAGACA 300
TRPV1b           GCACCAACCAGCTGGCCATTGTGAAGTTCCTGCTGCAGAACTCCTGGCAGCCTGCAGACA 250
                 ************************************************************

colony4          TCAGCGCCCGGGACTCAGTGGGCAACACGGTGCTTCATGCCCTGGTGGAGGTGGCAGATA 360
TRPV1b           TCAGCGCCCGGGACTCAGTGGGCAACACGGTGCTTCATGCCCTGGTGGAGGTGGCAGATA 310
                 ************************************************************

colony4          ACACAGTTGACAACACCAAGTTCGTGACAAGCATGTACAACGAGATCTTGATCCTGGGGG 420
TRPV1b           ACACAGTTGACAACACCAAGTTCGTGACAAGCATGTACAACGAGATCTTGATCCTGGGGG 370
                 ************************************************************

colony4          CCAAACTCCACCCCACGCTGAAGCTGGAAGAGATCACCAACAGGAAGGGGCTCACGCCAC 480
TRPV1b           CCAAACTCCACCCCACGCTGAAGCTGGAAGAGATCACCAACAGGAAGGGGCTCACGCCAC 430
                 ************************************************************
                                      EXON 6    EXON 8
colony4          TGGCTCTGGCTGCTAGCAGTGGGAAGATCGGGAAC-GTCATAA 522
TRPV1b           TGGCTCTGGCTGCTAGCAGTGGGAAGATCGGGAACCGTCAT-- 471
                 ********************************** *****
```

Figure 11. Sequence Data for TRPV1.b

Sequence data was generated using the Big Dye Terminator kit from Applied Biosystems. No Genbank entry exists for TRPV1.b from rat DRG. Therefore, cloned sequence (colony 4) was compared to the rat sequence missing the 180 nucleotides that constitute exon 7. ClustalW was used for all comparisons. Nucleotides highlighted in green represent the location of the forward primer. Nucleotides highlighted in red and blue represent the location of the reverse primer. Red nucleotides represent the 3' end of exon 6 and the blue nucleotides represent the 5' end of exon 8. The score column in the table above the alignment represents the similarity between the two sequences.

```
SeqA Name         Len(nt)  SeqB Name         Len(nt)  Score
==========================================================
1    TRPV1.beta   312      2    colony6      418      100
1    TRPV1.beta   312      3    colony3      471      100
2    colony6      418      3    colony3      471      99
==========================================================

                                                                  EXON 7
colony6         ATGATGCTCGAGCGGCC--CAGTGTGATGGATATCTGCAGAATTCGCCCTTGTTCTGGAG 58
colony3         --GATGCTCGAGCGGCCGCCAGTGTGATGGATATCTGCAGAATTCGCCCTTGTTCTGGAG 58
TRPV1.beta      ---------------------------------------------------GTTCTGGAG 9
                                                                   *********

                  EXON 8
colony6         AACCGTCATGACATGCTTCTCGTGGAACCCTTGAACCGACTCCTACAGGACAAGTGGGAC 118
colony3         AACCGTCATGACATGCTTCTCGTGGAACCCTTGAACCGACTCCTACAGGACAAGTGGGAC 118
TRPV1.beta      AACCGTCATGACATGCTTCTCGTGGAACCCTTGAACCGACTCCTACAGGACAAGTGGGAC 69
                *********************************************************

colony6         AGATTTGTCAAGCGCATCTTCTACTTCAACTTCTTCGTCTACTGCTTGTATATGATCATC 178
colony3         AGATTTGTCAAGCGCATCTTCTACTTCAACTTCTTCGTCTACTGCTTGTATATGATCATC 178
TRPV1.beta      AGATTTGTCAAGCGCATCTTCTACTTCAACTTCTTCGTCTACTGCTTGTATATGATCATC 129
                ************************************************************

colony6         TTCACCGCGGCTGCCTACTATCGGCCTGTGGAAGGCTTGCCCCCCTATAAGCTGAAAAAC 238
colony3         TTCACCGCGGCTGCCTACTATCGGCCTGTGGAAGGCTTGCCCCCCTATAAGCTGAAAAAC 238
TRPV1.beta      TTCACCGCGGCTGCCTACTATCGGCCTGTGGAAGGCTTGCCCCCCTATAAGCTGAAAAAC 189
                ************************************************************

colony6         ACCGTTGGGGACTATTTCCGAGTCACCGGAGAGATCTTGTCTGTGTCAGGAGGAGTCTAC 298
colony3         ACCGTTGGGGACTATTTCCGAGTCACCGGAGAGATCTTGTCTGTGTCAGGAGGAGTCTAC 298
TRPV1.beta      ACCGTTGGGGACTATTTCCGAGTCACCGGAGAGATCTTGTCTGTGTCAGGAGGAGTCTAC 249
                ************************************************************

colony6         TTCTTCTTCCGAGGGATTCAATATTTCCTGCAGAGGCGACCATCCCTCAAGAGTTTGTTT 358
colony3         TTCTTCTTCCGAGGGATTCAATATTTCCTGCAGAGGCGACCATCCCTCAAGAGTTTGTTT 358
TRPV1.beta      TTCTTCTTCCGAGGGATTCAATATTTCCTGCAGAGGCGACCATCCCTCAAGAGTTTGTTT 309
                ********************************************************

colony6         GTGAAGGGCGAATTCCAGCACACTGGCGGCCGTTACTAGTGGATCCGAGCTCGGTACCAA 418
colony3         GTGAAGGGCGAATTCCAGCACACTGGCGGCCGTTACTAGTGGATCCGAGCTCGGTACCAA 418
TRPV1.beta      GTG------------------------------------------------------- 312
                ***

colony6         ------------------------------------------------------
colony3         GCTTGGCGTAATCATGGTCATAGCTGTTTCCTGTGTGAAATTGTTATCCGCTC 471
TRPV1.beta      ------------------------------------------------------
```

Figure 12. Sequence alignment of cloned TRPV1.β sequences

Sequence data was generated using the Big Dye Terminator kit from Applied Biosystems. No Genbank entry exists for TRPV1.β from rat DRG. Therefore, cloned equences (colonies 3 and 6) were compared to rat sequences missing the final 30 nucleotides from exon 7. ClustalW was used for all comparisons. Nucleotides highlighted in green represent the location of the reverse primer. The nucleotides highlighted in red and blue represent the location of the forward primer, which straddles the truncated exon 7 and canonical exon 8. The red nucleotides are the 3' end of exon 7 and the blue nucleotides are the 5' end of exon 8. In this alignment, two cloned sequences were compared to the recorded sequence for TRPV1.β.

Quantification of TRPV1 mRNA and its splice variants in normal and CCI DRG

Quantitative PCR (qPCR) and the comparative CT method [97] were used to determine if the CCI treatment altered the mRNA expression of TRPV1, TRPV1.b, TRPV1.β, and TRPV1.var.

In total, 22 DRG, divided among the three treatment groups, were analyzed via qPCR. This number includes both the ipsilateral (right) and contralateral (left) level 5 DRG from each animal. For the sake of clarity, the term technical replicate must be defined before describing the comparative Ct method. The term technical replicate refers to the number of individual qPCR reactions conducted for a single gene using a single tissue sample as the source. In this case, 3 technical replicates and one no-template-control reaction were performed for each gene from each tissue sample. During the amplification stage of qPCR, the increase in amplicon concentration can be measured indirectly by the increase of fluorescence emitted by SYBR green. SYBR green is a dye that intercalates in between nucleotides in DNA molecules, and the DNA-dye complex will fluoresce when exposed to a 488nM wavelength. As the proportion of target cDNA is increased through PCR amplification, SYBR green has more targets to intercalate into and increase the fluorescence.

The comparative Ct method of quantification measures the change in mRNA expression of a gene of interest (GOI) relative to the mRNA expression of a control gene—a gene that is highly expressed and not subject to change in response to the treatment. Therefore, while the GOI is subject to change in response to the treatment, the control gene is not. In this experiment, Glyceraldehyde 3-phosphate dehydrogenase

(GAPDH) was used as the control gene. GAPDH is an important enzyme in glycolysis. During the course of the experiment, the fluorescence emitted by each gene will cross an arbitrarily chosen threshold. The cycle number at which the fluorescence breaks that barrier is referred to as the Ct value. Since the control gene should have a much higher initial concentration than the GOI, the cycle number (Ct value) at which it crosses the threshold will be much lower than the GOI, presuming that each gene comes close to the theoretical doubling that occurs during each cycle of PCR. Following each experiment, the 3 technical replicates for each GOI were averaged, as were the GAPDH technical replicates. See Figure 13 for an example of raw qPCR data. A ΔCt value for one gene from one tissue sample was calculated by subtracting the average Ct value for GAPDH from the average Ct value for the GOI. This is represented more clearly with the following formula:

$\Delta Ct = (\text{mean GOI Ct}) - (\text{mean GAPDH Ct})$, for one tissue sample.

Once the ΔCt values were calculated from all biological replicates for a single GOI, they were imported into an Excel spreadsheet. The next step in the comparative CT method is the calculation of ΔΔCt values. This is done by subtracting the ΔCt of an experimental sample (either CCI or sham) from the ΔCt of a control animal, which is represented by the following calculation:

$\Delta\Delta Ct = (\Delta Ct \text{ from Control animal}) - (\Delta Ct \text{ from Experimental animal})$

The significance of this value is that it represents a shift in cycle number of the GOI relative to GAPDH between the control sample and the experimental sample. If the value is positive, then the amount of starting DNA in the experimental sample is greater than in

the control sample, and if the value is negative, the opposite is true. The final step that must be taken to determine the relative change in gene expression is to transform the ΔΔCt value into fold-change values, which is done as follows:

$$\text{Fold Change} = 2^{(\Delta\Delta Ct)}$$

This value represents the change in expression of one experimental tissue sample (CCI or Sham) relative to one control tissue sample. In this experiment, 4 ipsilateral CCI, 4 ipsilateral Sham, and 3 ipsilateral control samples were focused on. To fully assess the effects of the procedure, a ΔΔCt value was generated for each CCI tissue by comparing it against each control tissue sample. Each sham sample was also compared to each control sample in the same manner. This combinatorial approach was done for each gene and gene isoform. Once all of the different ΔΔCt values were generated, the mean and standard deviation were calculated. These averaged values were then graphed to compare them to the control. Fold Changes for controls were calculated similarly to the others by generating ΔΔCt values for each control tissue sample relative to the other control tissue samples. A mean and standard deviation was calculated for this group as well.

Zeyzus [66] demonstrated that there was no significant difference in TRPV1 expression between control, sham, and CCI animals at day 9; they were not analyzed in this study. Similarly, her study did not find any significant difference in TRPV1 expression in DRG levels 3 or 4 at day 12, so they were not included in this analysis.

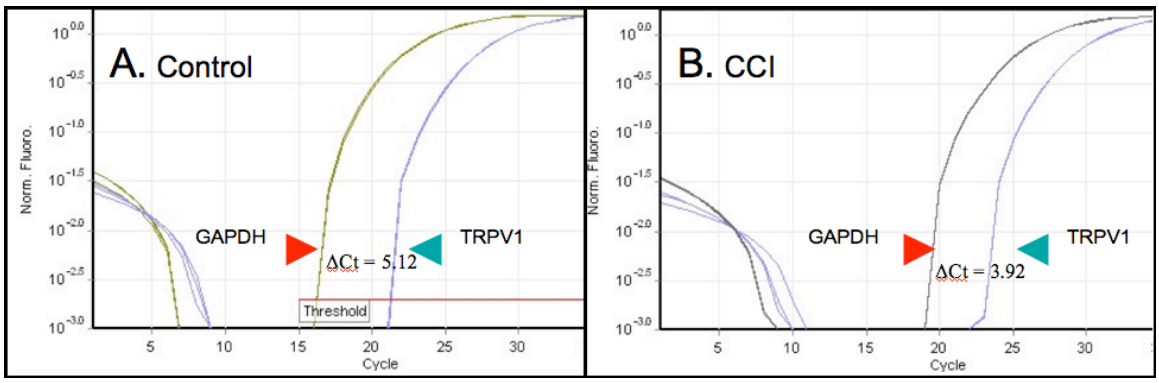

Figure 13. Quantitative PCR Data.

(A) Quantitative PCR plot generated using cDNA from a control ipsilateral L5 DRG. The red arrowhead is pointing at the triplicate curves of GAPDH and the turqoise arrowhead is pointing at the triplicate curves of TRPV1. The difference in cycle thresholds (ΔCt) is 5.12.
(B) Quantitative PCR plot generated using cDNA from a CCI ipsilateral L5 DRG. The red arrowhead is pointing at the triplicate curves of GAPDH and the turquoise arrowhead is pointing at the triplicate curves of TRPV1. The ΔCt is 3.92. The difference, or ΔΔCt, between 5.12 and 3.92 is 1.2. This value means that the starting amount of TRPV1 transcript in the CCI DRG is more than double that of the starting amount of transcript in the control DRG.

NPY and Gap43

For NPY, the data generated from trial 1 showed the greatest increase in expression in the CCI-treatment group. The first trial generated mean fold change values for the CCI-treatment, sham-treatment, and control groups of 64.20±33.79, 6.49±6.21, and 1.44±1.34, respectively (Figure 14A). These data show that the CCI-treatment group was significantly different from both the sham-treatment group and the control group ($p<0.001$). The sham-treatment group was not significantly different from the control group ($p>0.05$). For the second trial, the mean fold-change value for the CCI-treatment, sham-treatment, and control group were 43.38±34.37, 2.92±2.02, and 1.2±0.78, respectively (Figure 14B). Here, the CCI-treatment group was significantly different from the control group ($p<0.001$) and the sham-treatment group ($p<0.001$), but the sham treatment group was not significantly different from the control group ($p>0.05$).

For Gap43, the data from the first trial showed the greatest increase in expression for the CCI-treatment group. The mean fold-change values for the CCI-treatment, sham-treatment, and control groups were 2.42±0.32, 1.52±0.51, and 1.00±0.07, respectively (Figure 14C). These data show that the CCI-treatment group was significantly different from the sham-treatment and control groups ($p<0.05$). The sham-treatment group was not significantly different from the control group ($p>0.05$). For the second trial, the mean fold-change values for the CCI-treatment, sham-treatment, and control group were 1.90±0.85, 0.93±0.14, and 1.01±0.20, respectively (Figure 14D). Here, the CCI-treatment group is not significantly different from the control group or from the sham-treatment group ($p>0.05$). The sham-treatment group is not significantly different from the control group. Though not significantly different from the sham-treatment or control

group, the CCI-treatment group has a much greater mean fold-change value, and is close to being significantly different ($p=0.072$).

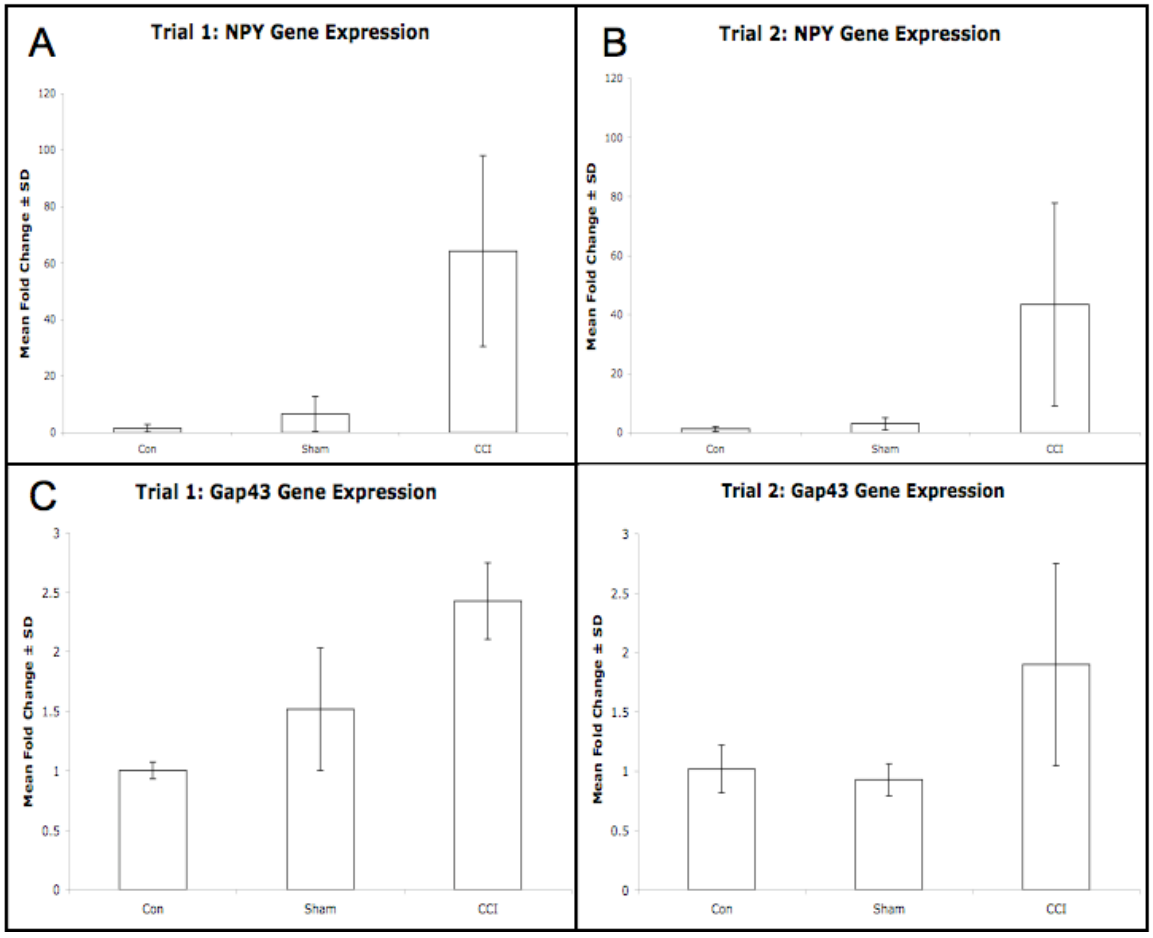

Figure 14. Relative NPY and Gap43 Expression 12 days Post-Surgery using cDNA as Template Material

(A) Trial one analysis of NPY using polyA primed cDNA. NPY expression from the CCI-treatment group showed a 62.74-fold increase relative to the control group and a 57.7-fold increase in expression relative to the sham-treatment group. These values are highly significant.
(B) Trial two analysis of NPY using polyA cDNA. NPY expression from the CCI-treatment group showed a 42.2-fold increase in expression relative to the control group, and a 40.5-fold increase in expression relative to the sham-treatment group. These values are highly significant.
(C) Trial one of Gap43 analysis using polyA primed cDNA. Gap43 expression from the CCI-treatment group showed a 1.4 fold increase in expression relative to the control and a 0.9 fold increase in expression relative to the sham-treatment group. Both comparisons are significantly different.
(D) Trial two of Gap43 analysis using polyA primed cDNA. Gap43 expression from the CCI-treatment group showed a 0.89-fold increase in expression relative to the control group and a 0.98-fold increase in expression relative to the sham-treatment group. Neither comparison was significantly different, although the trend supports the data from the first trial.

Expression of TRPV1 from DRGs removed 12 Days post-surgery

We first measured TRPV1 mRNA expression by using reverse-transcribed cDNA as the template material. The results we got using this method were poor and unreliable, and we believe that using cDNA as the template material was an incorrect choice. We then measured TRPV1 expression was measured by using mRNA as the starting material. The results using this method were much better and support our hypothesis that the CCI surgery increases TRPV1 expression. The qPCR data generated using mRNA as the starting material also suggest that the rats experienced mirror pain.

Analysis of cDNA generated by polyA priming

Two separate trials of analysis were conducted for each primer set using cDNA as the template material. For each trial, an independently generated pool of cDNA was generated. To prime the reverse-transcription process, primers that target the polyadenosine tail of mRNA were used. These primers are not gene specific and will anneal to all mRNA. For each trial, TRPV1 expression was measured once with both the Qiagen machine and the Applied Biosystems machine. This resulted in four sets of data (Figure 15). Unless otherwise stated, all comparisons are between the ipsilateral mean fold change value of the CCI-treatment group to the ipsilateral mean fold change value of the sham-treatment and control groups.

The results from the first trial using polyA primed cDNA generated by the Qiagen machine (Figure 15C) were the only ones that were consistent with the results generated by Zeyzus [66]. Though not significantly different from the control animals, the CCI animals had a mean fold change value almost 200% greater than the control. Likewise,

there is no significant difference in expression between the CCI animals and the sham animals, although the mean value for the CCI animals is greater. The mean fold change value for the sham animals was somewhat elevated. There was more variance in the control animals than expected. The mean fold change values for the CCI-treatment, sham-treatment, and control groups are 2.96±3.23, 2.06±2.08, and 1.37±1.18, respectively.

The second trial using polyA primed cDNA and the Qiagen machine did not corroborate the trend observed in the first trial (compare Figure 15C with Figure 15D), nor the data generated by Zeyzus [66]. The mean fold value for the CCI-treatment, sham-treatment, and control groups were 0.65±0.24, 1.54±1.13, and 1.02±0.20, respectively (Figure 15D). No significant differences between the groups exist.

The second trial using polyA primed cDNA and the Applied Biosystems machine was similar to that of the second trial using the Qiagen machine (compare Figure 15A with Figure 15B). No significant changes in expression were observed in either the CCI or sham groups. The mean values for the CCI and Sham animals were actually slightly lower than the control group, which itself was slightly higher than expected. The mean fold change values for the CCI-treatment group, sham-treatment group, and control group were 0.94±0.40, 0.94±0.47, and 1.14±0.62, respectively (Figure 15A).

The second trial using polyA primed cDNA and the Applied Biosystems machine was the least informative as it showed that all three treatment groups being elevated, and the sham-treatment group having the greatest mean fold value. The mean fold value for the CCI- treatment group, sham-treatment group, and control group are 2.88±2.87,

4.70±5.90, and 1.96±2.43, respectively (Figure 15B). Again, these data were not significantly different from each other.

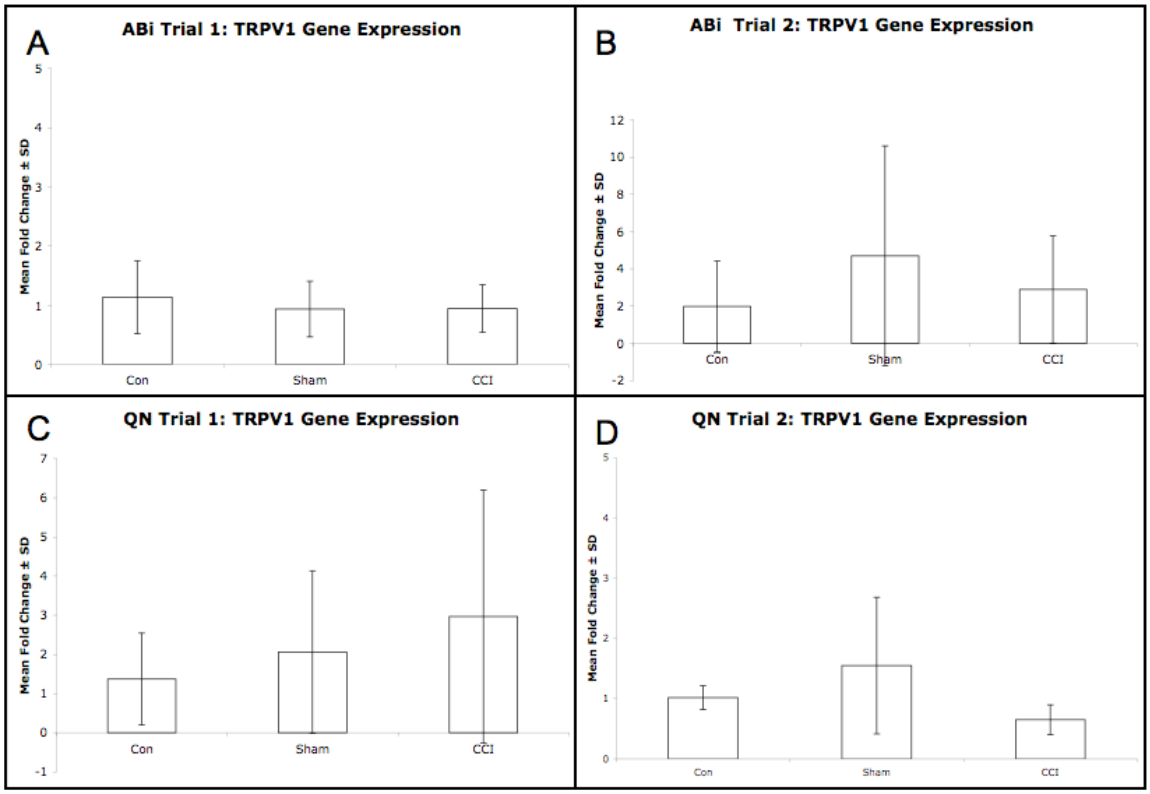

Figure 15. Relative Gene Expression of TRPV1 using cDNA as Template Material

(A) Trial 1 analysis using polyA primed cDNA and the Applied Biosystems Machine. TRPV1 expression in the CCI-treatment group is not significantly different from either the sham-treatment group or the control group. Likewise, the mean fold change values are all very similar.
(B) Trial 2 analysis using polyA primed cDNA and the Applied Biosystems machine. TRPV1 expression is not significantly different from either treatment group. The mean fold change values for the sham-treatment and CCI-treatment are elevated though.
(C) Trial 1 analysis using polyA primed cDNA and the Qiagen machine. TRPV1 expression in the CCI-treatment group is not significantly different from either the sham-treatment group or the control group. The mean fold change value for the CCI-treatment group is highest in this set of experiments.
(D) Trial 2 analysis using polyA primed cDNA and the Qiagen machine. TRPV1 expression in the CCI-treatment group is not significantly different from either the sham-treatment group or the control group. The mean fold change value is lower than the control, which would suggest expression has decreased.

TRPV1 expression using mRNA as the template material

Because the qPCR data using polyA primed cDNA were inconclusive, qPCR experiments were performed using mRNA as the template material. This form of qPCR analysis is different because the reverse-transcription and amplification steps are not separated. It also utilizes gene specific primers instead of the nonspecific poly(dT) primers which target the polyA tail of all mRNA transcripts. Using gene-specific primers results in only the reverse transcription and amplification of a single target. The number of technical replicates performed for each tissue sample varied, depending on the remaining amount of RNA available. As a consequence, it was impossible to run 3 technical replicates for TRPV1, TRPV1.b, and GAPDH for all tissue samples. The data generated from the 1-step experiment support the hypothesis that the CCI surgery increases the expression of TRPV1. The 1-step data also resemble the first trial data generated using the Qiagen machine. The mean fold value for the CCI group was almost triple the Control, and the Sham mean value was twice as great as the control group. The mean fold change value for the CCI-treatment group, sham-treatment group, and control group were 2.60±1.25, 2.06±1.04, and 1.10±0.50, respectively. Neither treatment group was significantly different from control group, or each other. See Figure 16 for details.

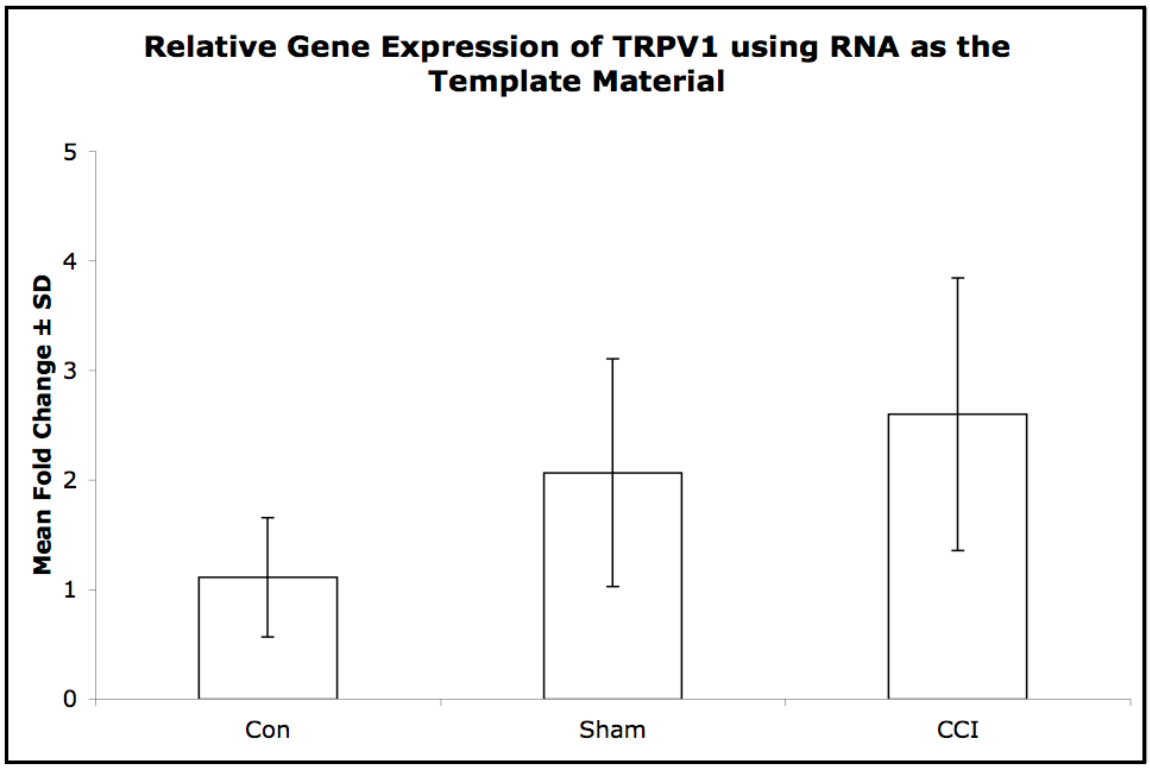

Figure 16. Relative Expression of TRPV1 using RNA as Template Material

Bars represent the mean fold change ± standard deviation (SD) of TRPV1 expression. The CCI procedure increased TRPV1 expression 2.6 fold relative to the control group. The sham surgery increased TRPV1 expression 2.06 fold relative to the control group. The CCI-treatment group was not significantly different from either the sham-treatment group or the control group ($p=0.087$). The sham-treatment group was not significantly different from the control group. The Applied Biosytems machine was used for this analysis.

Results from direct amplification of TRPV1 mRNA suggest mirror pain in CCI treated rats.

An interesting finding of this analysis is that a mean-fold comparison of the ipsilateral versus contralateral DRG samples for the CCI-treatment group shows them to not be significantly different (0.78±0.31). The mean ΔCt values for each group are also similar to one another (ΔCt Ipsilateral = 3.15, Contralateral = 2.70). This suggests that both sides of the CCI-treatment animals experienced an increase in TRPV1 expression. Both sides also have mean ΔCts lower than either the sham-treatment or control groups. Mirror pain is a phenomenon where a unilateral injury causes bilateral pain [98].

Relative gene expression of TRPV1 splice variants 12 days post-surgery

Using primers that target individual splice variants, it was demonstrated that TRPV1.var, TRPV1.β, and TRPV1.b exist in rat DRGs. Using cDNA as template material, it was found that the mean fold values for TRPV1.b were elevated in sham and CCI animals, but were not significantly different from the control animals. Using mRNA as template material, TRPV1.b expression in the CCI-treatment, sham-treatment, and control group was unchanged and non-significant. Expression of TRPV1.β was slightly elevated in sham and CCI animals using cDNA, but was not significantly different. TRPV1.var expression in CCI animals was relatively unchanged, if not lower than the control animals.

TRPV1.b

TRPV1.b was the first variant examined in this study. It is a splice variant of TRPV1 that is generated through the removal of the entire seventh exon. Like TRPV1,

its expression was analyzed using both the Qiagen machine and the Applied Biosystems machine. The four trials suggest as a group that both the chronic constriction injury procedure and the sham surgery increase the expression of TRPV1.b. These trials also showed a great amount of variation within treatment groups, making any analysis less precise.

The first trial of TRPV1.b using polyA primed cDNA with the Qiagen machine shows a 100% increase in expression in the CCI-treatment group, and a 300% increase in expression in the Sham-treatment group. The mean fold-change value for the CCI-treatment group, sham-treatment group, and control group are 2.06±1.32, 3.55±1.24, and 1.06±0.37, respectively (Figure 17C). The sham-treatment group is significantly different from the control group, but not from the CCI-treatment group. The CCI-treatment group is not significantly different from either of the other groups.

The second trial using the Qiagen machine was different from the first trial. Here, the mean fold-change value for the CCI-treatment group, sham-treatment, and control group are 7.66±8.09, 22.86±32.24, and 1.00±0.03, respectively (Figure 17D). The CCI-treatment group was not significantly different from either the sham-treatment or control groups. The sham-treatment group was not significantly different from the control group.

The reason for such large mean fold changes in the CCI-treatment and the sham-treatment groups is that there was a large amount of variation in the ΔCt values. For the sham-treatment group, the four ΔCts were 1.21, 3.47, 6.9, and 8.47. The 1.21 ΔCt value is responsible for skewing the sham-treatment group. If that low Ct value is excluded from the analysis, then the mean fold value for the sham-treatment group becomes 5.80±7.50. The 4 ΔCt values for the CCI-treatment group are 3.16, 6.62, 4.15, and 11.15.

If the 11.15 ΔCt is excluded, then the mean fold value for the CCI-treatment group becomes 10.18±7.81. An additional problem that made this one set of experiments difficult is that no ΔCt value was generate for one control rat, meaning all fold change values were generated using only the two remaining control animals. There was very little variation between the two control animals. Their ΔCt values were 7.45 and 7.39.

The first trial using the Applied Biosystems machine found no significant difference between the mean fold change values of the three treatment groups. The mean fold value for the sham-treatment group was especially high in this set of data too. In this data set, the same sham-treatment animal that skewed the data in the previous data set also skews the data in this one. The four ΔCts for the sham-treatment group are 6.53, 9.38, 9.15, and 10.13. The mean fold change for the CCI-treatment group, sham-treatment (including all samples), and control group are 1.39±1.07, 4.40±6.44, and 1.39±1.24, respectively (Figure 17A). If the one sham animal is removed, then the mean fold value for the sham-treatment group becomes 1.63±1.15.

The second trial using the Applied Biosystems machine for TRPV.b showed that the the CCI-treatment group experienced an increase in expression, similar to that of the data generated by the first trial using the Applied Biosystems machine. The mean fold change for the CCI-treatment group, sham-treatment group, and control treatment group are 11.46±10.71, 52.69±82.43, and 1.03±0.29, respectively (Figure 17B). The cause for the high mean fold value of the sham-treatment group is the same sham animal as from the second trial using the Qiagen machine. When it is removed from the analysis the mean fold change for the sham-treatment group becomes 8.44±11.02.

TRPV1.b was also analyzed using the 1-step qPCR technique, where RNA instead of cDNA is used as the template. Like the 2-step data, the 1-step data found that there are no significant differences between the CCI-treatment, sham-treatment, and control groups. The mean fold change values for the CCI-treatment, sham-treatment, and control groups are 1.33±0.55, 1.42±1.045, and 1.55±1.59, respectively (Figure 18). There were no wild ΔCt values in the sham-treatment group for this analysis. This may suggest that the problem stemmed from the reverse-transcription process used to generate the cDNA for the 2-step analyses.

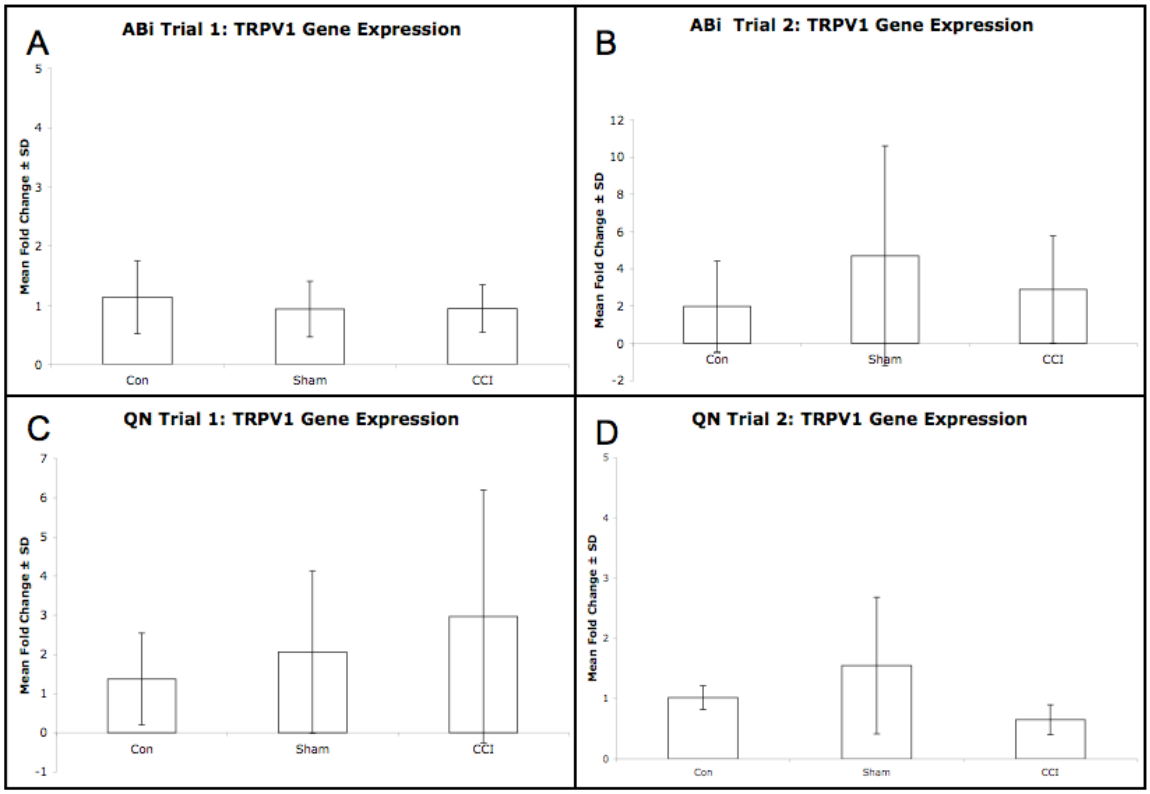

Figure 17. Relative Gene Expression of TRPV1.b using cDNA

(A) Trial one using polyA primed cDNA, TRPV1.b expression from the CCI-treatment group was not significantly different from either the sham-treatment group or the control group. The mean fold value for the sham-treatment group was elevated relative to the other groups, but was not significantly different. N = 3 for control group, N = 4 for the sham-treatment group, and N= 4 for the CCI-treatment group.
(B) Trial two using polyA primed cDNA, TRPV1.b expression from the CCI-treatment group was not significantly different from either the sham-treatment or control group. The mean fold value for the sham-treatment group was much higher than either group, but was not significantly different. The high value is due to a single sham-treatment sample having very high ΔΔCt values. N = 3 for control group, N = 4 for the sham-treatment group, and N= 4 for the CCI-treatment group.
(C) Trial one using polyA primed cDNA, TRPV1.b expression from the CCI-treatment group was not significantly different from either the sham-treatment group or control group. The sham-treatment group was 2.5-fold greater than the control group and is significantly different. The mean fold change for the CCI-treatment group is 2.8-fold greater than the control group, but not significant. N = 3 for control group, N = 4 for the sham-treatment group, and N= 4 for the CCI-treatment group.
(D) Trial two using polyA primed cDNA, TRPV1.b expression from the CCI-treatment group is not significantly different from either the sham-treatment group or the control group. The mean fold values for the sham-treatment group and CCI-treatment group were 21.6-fold and 6.6-fold greater than the control group, but were not significant. N = 2 for control group, N = 4 for the sham-treatment group, and N= 4 for the CCI-treatment group.

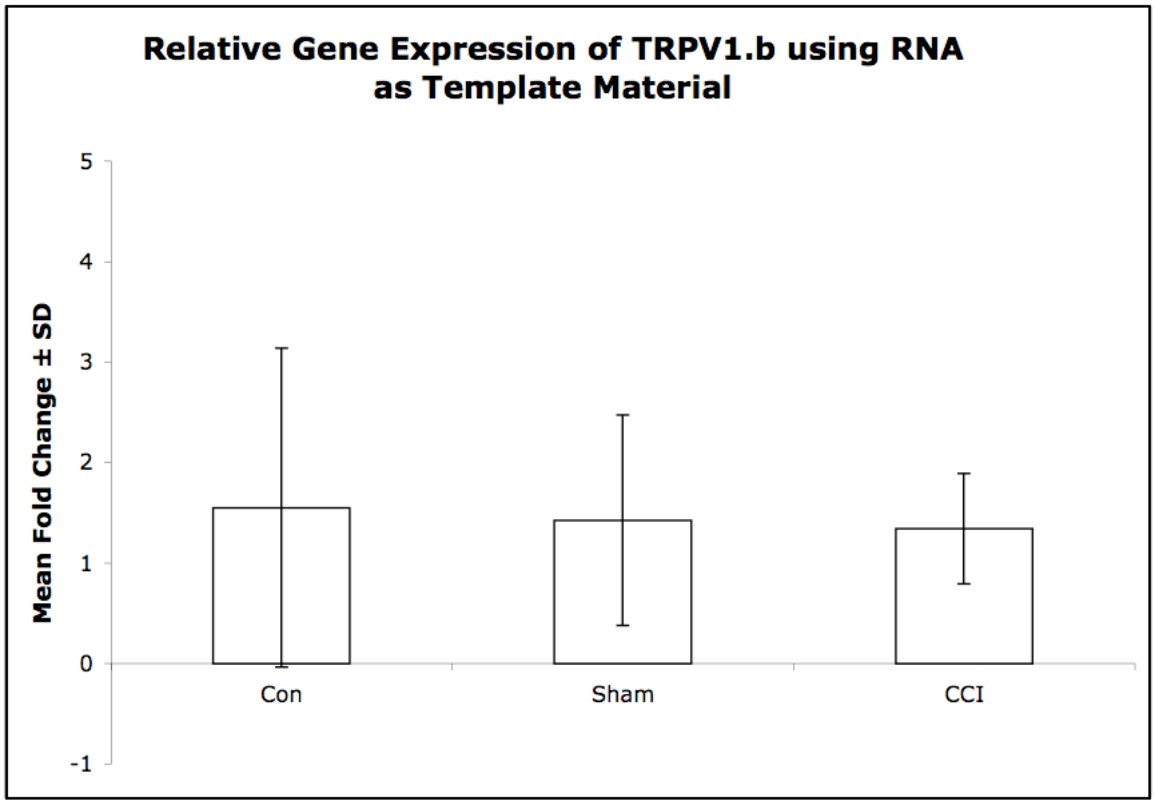

Figure 18. Relative Gene Expression of TRPV1.b using mRNA

Using mRNA as the template material, TRPV1.b expression from the CCI-treatment group was not significantly different from either the control group or the sham-treatment group. The mean fold change for the sham-treatment and CCI-treatment were also not elevated relative to the control group. N = 3 for control group, N = 4 for the sham-treatment group, and N= 4 for the CCI-treatment group.

TRPV1.β

TRPV1.β is an isoform of TRPV1 that is generated through the use of a cryptic 5' splice site that truncates the seventh exon by 30 base pairs. With primers that target TRPV1.β, I was unable to demonstrate in either trial that its expression was significantly altered by either the sham or CCI surgery. Only the Applied Biosytem machine was used for this analysis. For the first trial, the mean fold change values for the CCI-treatment, Sham-treatment, and Control groups were 0.91±0.54, 2.48±1.90, and 1.01±0.21, respectively (Figure 19A). There was also no difference in expression between the ipsilateral and contralateral sides of the CCI-treatment and sham-treatment groups. There was a slight increase in expression of the ipsilateral side relative to the contralateral side in the control group (1.92±0.50).

The second trial using polyA primed cDNA for TRPV1.β differed from the first trial. The mean fold change values for the CCI-treatment, sham-treatment, and control groups were 3.06±3.46, 2.30±2.54, and 1.09±0.48, respectively (Figure 19B). There were no significant differences for the ipsilateral versus contralateral comparisons for the CCI-treatment, sham-treatment, and control groups.

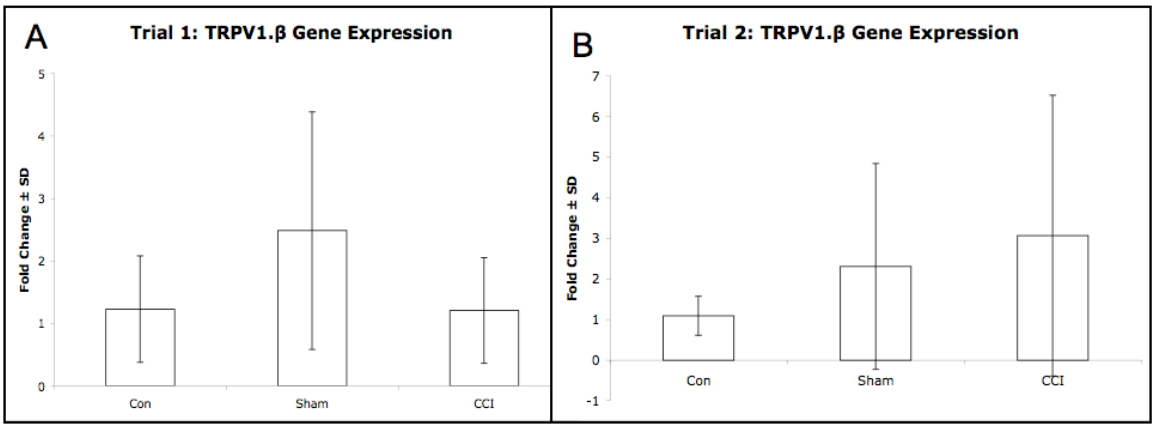

Figure 19. Relative Gene Expression of TRPV1.β

(A) Trial one. TRPV1.β expression from the CCI-treatment group was not significantly different from either the control group or the sham-treatment group. The mean fold value for the sham-treatment group was elevated, surprisingly, but was not significantly different. N = 3 for control group, N = 4 for the sham-treatment group, and N= 4 for the CCI-treatment group.
(B) Trial two. TRPV1.β expression from the CCI-treatment group was not significantly different from either the control group or the sham-treatment group. The CCI-treatment group did have an elevated mean fold value relative to the control group, but it was not significant. N = 3 for control group, N = 4 for the sham-treatment group, and N= 4 for the CCI-treatment group.

TRPV1.var

TRPV1.var is an isoform of TRPV1 generated through the retention of the intron between exons 5 and 6 and usage of an alternative start site. Using primers that target TRPV1.var, I was unable to demonstrate that its expression was significantly altered by either the sham or CCI procedures, in either trial one or two. For the first trial, the mean fold change for CCI, Sham, and Control were 1.19±1.13, 6.75±9.39, and 1.76±2.02, respectively (Figure 20A). For both the CCI-treatment and sham-treatment groups, a single rat had a Ct value 2 cycles lower than the other rats. Removing that one rat from either group lowers the mean fold values of the CCI group, and the sham group to 0.78±0.60 and 2.71±2.76, respectively.

For the second trial, the mean fold change for the CCI-treatment, sham-treatment, and control groups were 1.12±1.40, 1.28±1.18, and 1.20±0.77 (Figure 20B). One rat in the CCI-treatment group did have a ΔCt 2.5 cycles lower than the others (9.94 vs. 12.48, 13.05, and 13.08). Eliminating that one value from the CCI-treatment group had a large effect on the mean fold change value for that group, changing it from 1.12±1.40 to 0.42±0.19. The other two groups did not have outliers like the CCI-treatment group.

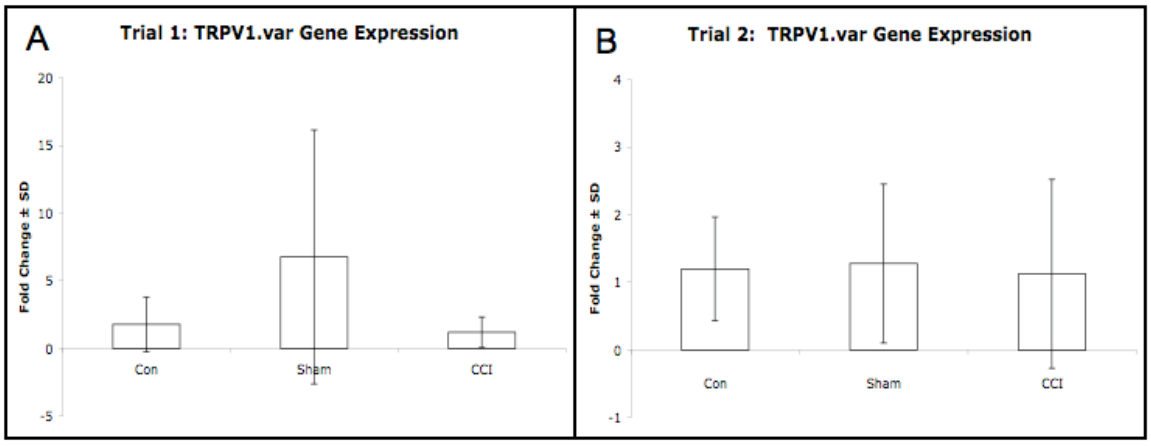

Figure 20. Relative mRNA Expression of TRPV1.var

(A) Trial one using polyA primed cDNA, TRPV1.var expression from the CCI-treatment group was not significantly different from either the control group or the sham-treatment group. Likewise, the mean fold change values for the sham-treatment and CCI-treatment groups were not very different from the control group.
(B) Trial two using polyA primed cDNA, TRPV1.var expression from the CCI-treatment group was not significantly different from either the control group or the sham-treatment group. Surprisingly, the mean fold change value for the sham-treatment group was elevated, though not significantly different.

Immunohistochemistry and confocal microscopy

The results from this experiment show that an increase in TRPV1 expression can be observed in level 5 DRGs, 12 days post-CCI. To characterize the expression of TRPV1 in vivo, we analyzed sections of level 5 DRG from CCI treated and control rats with antibodies against TRPV1 and Neurofilament-M. Additionally, the plantar region of the right rear paw of each rat was injected with DiD, a retrograde fluorescent dye. DiD will only stain the neurons innervating that specific region of the foot. In several sections, we observed robust fluorescence from medium (500-1000μm^2) diameter neurons, stained with both NFM and TRPV1. The average area of these 5 cells is 795 μm^2. As expected, not all neurons were positive for the DiD tracer since only a discrete number of neurons reach the footpad. However, in one tissue section, we observed robust fluorescence from neurons stained with NFM, TRPV1, and DiD (Figure 21A). Leica confocal software was used to analyze the expression of neurons positively stained for TRPV1 in the L5 DRG from the CCI treated rat and the Control rat. The results show increased TRPV1 expression in neurons from CCI affected DRGs (Figure 21B).

Figure 21. Anti-TRP Immunohistochemistry and Comparison of Relative Fluorescence for Normal Versus CCI Cells.

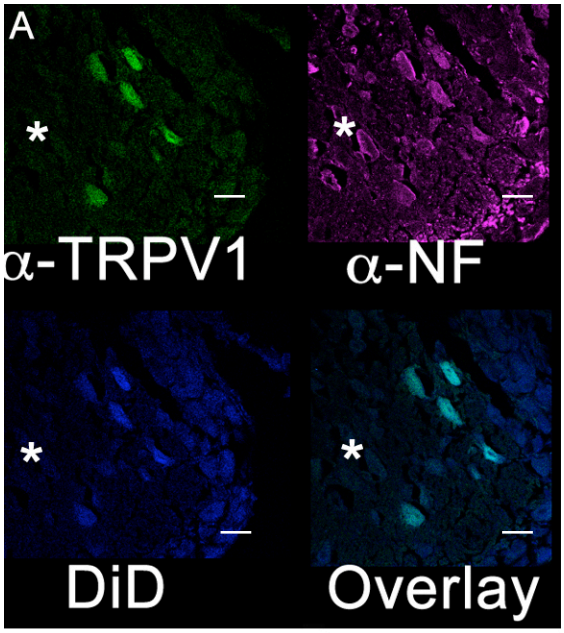

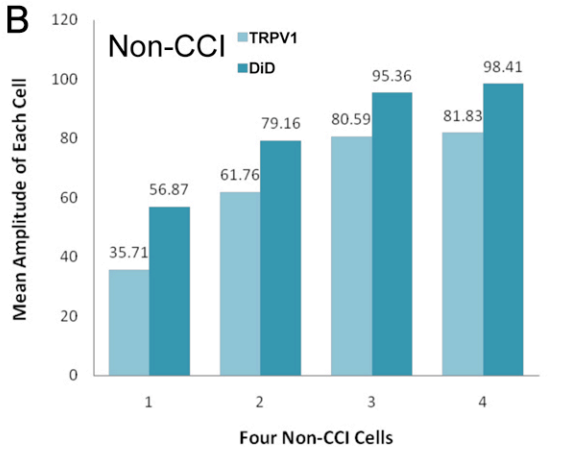

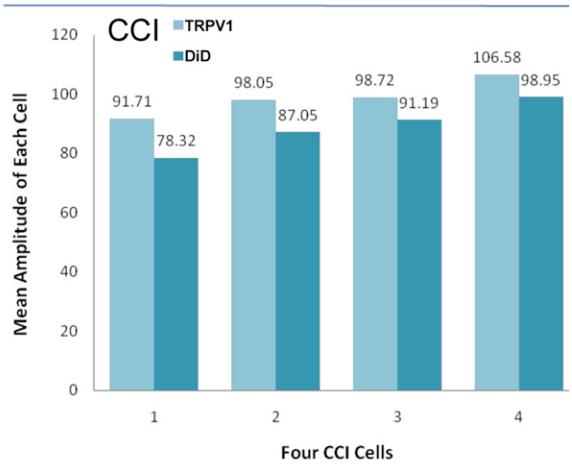

C

Non CCI	Overall Mean Amplitude of all Four Cells
TRPV1	64.97
DiD	82.45
Overall TRPV1 Mean Amplitude / Overall DiD Mean Amplitude	.787

CCI	Overall Mean Amplitude of all Four Cells
TRPV1	98.77
DiD	88.88
Overall TRPV1 Mean Amplitude / Overall DiD Mean Amplitude	1.12

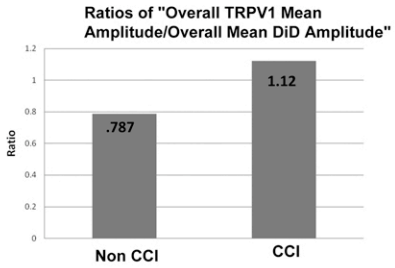

Figure 23. A. DiD retrogradely labeled DRG were processed for multi-stain confocal microscopy with anti-TRPV1 and anti-Neurofilament antibodies. The results reveal that some neurons co-label with TRPV1 and DiD, while other neurons (*) lack both. Scale bar is 40μm^2 **B.** Using Leica confocal software, we measured the relative fluorescence of TRP to DiD for representative CCI and control cells. **C.** Summary of the relative fluorescence of TRPV1 shows that its expression is increased in CCI DRG.

Chapter 4

DISCUSSION

Summary

Transient Receptor Protein Vanilloid 1 (TRPV1) is an ion channel that responds to capsaicin, the molecule that imparts chili peppers with their fiery taste. It is also a protein that integrates mechanical and thermal sensations, and is involved in nociception [35,60,99]. The surgical procedure used in this study is called chronic constriction injury (CCI). It is a procedure designed to model the human neuropathic pain condition called Complex Regional Pain Syndrome II. The CCI procedure was designed by Bennet and Xie in 1988 [92]. Previous reports on TRPV1 expression have demonstrated that nerve injuries increase its protein and mRNA expression. The present study set out with two primary goals. The first was to confirm that the TRPV1 expression is elevated in lumbar level 5 DRG ipsilateral to the CCI surgery of the sciatic nerve. The second was to demonstrate that the CCI procedure alters the relative expression of three TRPV1 splice variants: TRPV1.var, TRPV1.b and TRPV1.β.

I have found that CCI did not cause an increase in thermal hyperalgesia and mechanical allodynia at day 12 post-surgery. I did demonstrate that neuronal trauma took place only in the CCI group by analyzing the expression of two positive control genes, NPY and Gap43, consistent with previous studies [100,101]. I was unable to demonstrate that TRPV1 expression is significantly higher in the CCI treatment group, but the mean fold value is greater than either the control group or sham-treatment group. The

expression of splice variant TRPV1.b is elevated in sham and CCI-treatment groups when cDNA is used for template material, but is not significantly different. TRPV1.β and TRPV1.var expression is unaffected by the CCI surgery.

Quantification of TRPV1 mRNA and its splice variants mRNA following CCI surgery

TRPV1

The results of this study show that there are no statistically significant differences in expression of TRPV1 between the CCI-treatment group and the sham-treatment group. That is, I am unable to demonstrate that the neuropathic pain model, CCI, was able to increase the expression of TRPV1 in total DRG in a way that was unique from the non-neuropathic sham surgery, which did not include the ligation of the sciatic nerve. This was true using both the Applied Biosystems real-time PCR machine and the Qiagen machine, and it was true for the studies using cDNA and mRNA. That said, the experiments using mRNA did result in a mean increase in expression of TRPV1 by 2.60±1.25 fold in the CCI-treatment group, which is 0.54 fold greater than the mean increase of expression of the sham-treatment group (2.06±1.04). The studies using cDNA, however, were inconsistent and cannot statistically indicate that the CCI treatment was significantly different from the sham treatment. These data are also consistent with the behavioral data, which showed that there were no increases in mechanical allodynia or thermal hyperalgesia in the CCI treated rats.

The mean fold increase reported here for the CCI-treatment group is consistent, and somewhat greater, than the mean fold increase reported by Zeyzus [66]. In her report, she found that mean TRPV1 expression from day 12, lumbar level 5 DRG

ipsilateral to CCI was 1.6-fold greater than control expression, which is 1.0 fold lower than the mean fold value for this study. She also reported a mean 1.5 fold increase of TRPV1 expression in the ipsilateral DRG of CCI rats relative to the contralateral DRG of the same rats. In the sham-treatment and control group, she found no difference in expression. In this study, the data suggest that the CCI-treated rats had an increase in expression in both the ipsilateral and contralateral DRG. The ipsilateral DRGs of the CCI animals relative to the contralateral DRGs had a mean fold change of 0.78±0.31, which is not statistically significant, but is the opposite of the results presented by Zeyzus [66]. It is an interesting finding and would suggest that the animal experienced allodynia and hyperalgesia in the unaffected paw, which is referred to as mirror pain. No evidence from the behavioral data supports that position. This finding is discussed in greater length below.

The lack of statistical significance was surprising since it has been previously shown that CCI and other pain models do induce an upregulation of TRPV1 protein and mRNA expression [62,63,102,103,104]. Other studies, however, have also found that neuropathic pain models do not cause an upregulation of TRPV1. A study in 2007 showed similar results to those found here. That study, by Frederick et al. [105], found no significant increase in TRPV1 following CCI 7 and 14 days post-surgery. Their hypothesis for why TRPV1 transcript levels were unchanged following CCI is that TRPV1 expression is controlled by unspecified post-transcriptionally regulated events. Another study by Michael and Priestley (1999) showed that TRPV1 expression in DRGs is actually decreased following sciatic nerve ligation [106]. Similar to the study by Michaels and Priestley, a study by Hudson et al. [62] found that TRPV1 expression

decreased in DRG neurons damaged by total or partial nerve ligation. They did find that TRPV1 expression was increased in the remaining undamaged neurons.

Given the context of these other studies, it may be the case that the sutures tied around the sciatic nerves of the rats in this study were too tight, damaging a subset of neurons and diminishing the TRPV1 expression. No post-mortem analyses of the sciatic nerves in this study were performed, so it is impossible to determine if the CCI surgery was done correctly, or if over-tightening or full ligation occurred. My personal belief is that over-tightening probably did occur in at least one animal. The previous studies analyzed mRNA expression or protein expression using antibodies or oligonucleotide probes against fixed DRG sections, allowing them to analyze individual neurons. I analyzed TRP expression in homogenized tissue samples, so any increase in expression from uninjured neurons may have been diluted by the RNA from the injured neurons.

This study also used a small number of animals. As a consequence, the over-tightening of sutures in one animal may drastically affect the final expression data. Only 11 animals total were used, 4 in the CCI-treatment group, 4 in the sham-treatment group, and 3 in the control group.

Quantification of splice variants of TRPV1

The second objective of this study was to determine the effects of the chronic constriction injury procedure on the expression of TRPV1 splice variants. To our knowledge, this is the first time that the effects of CCI on TRPV1.b, TRPV1.β, and TRPV1.var have been studied. Each of these three splice variants are similar in that they each undergo alternative splicing within the N-terminal region of the gene.

I found that there were no statistically significant differences between the CCI- and sham-treatment groups with respect to TRPV1.β, TRPV1.b, and TRPV1.var. The TRPV1.b data, however, appear to trend upward in the CCI-treatment group. Three of the four analyses using cDNA found that TRPV1.b had increased mean fold change values, indicating an elevation in expression relative to control. These are not supported by the study using mRNA though. The mean fold value was greatest from trial 2 using both the Applied Biosystems machine and the Qiagen machine.

TRPV1.b is a splice variant of TRPV1 that was first identified in human brain tissue. It is generated through the excision of exon 7 from pre-mRNA. TRPV1.b is similar to the canonical transcript in every other respect. To isolate TRPV1.b, I used primers that were published in a paper by Charrua et al. [83]. The forward primer is complementary to both the variant and the canonical transcript. The reverse primer is the one that isolates TRPV1.b, as it is complementary to the last 9 nucleotides of exon 6 and the first 9 nucleotides of exon 8. Of the 4 analyses that were conducted using cDNA as the template material, 3 showed TRPV1.b expression increasing in the CCI-treatment group. These values ranged from a 2-fold increase to a 11-fold increase. In all cases, these values were not statistically different from the control group or the sham-treatment group, as the standard deviations were very large.

The results for TRPV1.b, of the three, are perhaps the most interesting because they fail to corroborate the data generated by Charrua et al. [83]. In their study, they found that cyclophosphamide injection-evoked cystitis significantly downregulates TRPV1.b but does not alter the expression of TRPV1. A number of possible reasons could contribute to the differences in findings. The first reason is that they used a

different pain model in their attempt to alter the expression of TRPV1 and TRPV1.b. The second difference is that for their analysis they combined mRNA from lumbar level 5 and 6, whereas I only used level 5 for my source of RNA. Depending on the number of neurons from those two DRGs that innervate the bladder, they might be working with a larger population of neurons that experience changes in expression than I do. The third reason is that they did their analyses 1 day and 3 days after they injected their irritant into the rats, whereas I did all of my analyses on tissue samples 12 days post-operation. Another possible explanation is the set of primers that was used to quantify TRPV1.b. Normally, primers designed for qPCR generate amplicons between 75 and 150 base pairs in length. The primers designed by Charrua et al. that target TRPV1.b generate an amplicon of 471 base pairs, over three times the length suggested by Applied Biosystems. The length can impact the efficiency of the cycling, introducing unwanted variation into the ΔΔCt analysis. And, unlike primers designed for canonical sequences, these primers can only target a specific set of nucleotides since the splice event is a deletion. This results in a primer set that may be less efficient than desired, which is probably the case in this study.

It's also possible that the discrepancies between the analyses using cDNA are a result of the reverse-transcription process. The reverse transcriptase enzyme used in the process does not have as great of a processitivity as any other polymerase, so when reverse transcribing longer transcripts, it is more likely to fall off before generating a full length cDNA molecule. The problem arises because the splicing events all occur in the 5'-region, which is farthest away from the polyadenosine tail, and is where the primers bind to initiate reverse-transcription. Even though each reverse-transcription reaction

started with the same amount of total RNA, it is possible that the distribution of TRPV1.b mRNA was not even, so the resultant product would not be uniform. Though the data generated using mRNA shows no change in expression, which is different from the studies using cDNA, it still does not support the conclusion drawn by Charrua et al. Combined with the lowered processitivity, some of the variation between analyses can be explained.

During the course of the TRPV1.b experimentation, a problem was detected that affects all conclusions concerning it. That problem is the fact that the seventh exon is spliced out in both TRPV1.b and TRPV1.5'sv. This means that the primers used in this study cannot differentiate between the two isoforms, so no conclusion can be made about just one or the other. The consequence of this ambiguity is that it is difficult, if not impossible, to say with certainty whether or not the TRPV1.b alone is being studied. This problem was not reported in the Charrua et al. paper. The significance of splicing in the N-terminal region is discussed in below.

TRPV1.β is a splice variant of TRPV1 that was first isolated in DRGs from C57BL/6 mice. It is generated through the use of a cryptic 5' splice site that truncates the end of exon 7 by 30 base pairs. To analyze its expression, I generated primers that span the new exon-exon junction between the truncated exon 7 and the canonical exon 8. The results of the 2 analyses using cDNA as the starting template are not consistent. The mean fold value for the CCI-treatment group generated during trial 1 shows no change in expression relative to the control group, whereas the mean fold change generated during trial 2 shows a mean fold value 3.06. Both analyses are not significant though, since the standard deviations of each are very large. The mean fold values for the sham-treatment

group are actually similar to each other, differing by only 0.2 fold. They are both also elevated above the control group, and neither of them is significantly different from the control groups. All of the problems regarding primers and reverse-transcription that were discussed above also apply to TRPV1.β. Despite those caveats, the conclusion that I must draw from these data is that TRPV1.β expression is not affected by CCI. No other studies have been published that have analyzed its expression, so I have nothing to compare my results to.

TRPV1.var is an isoform of TRPV1 that was first identified in rat renal papilla cells by Tian et al. [78]. Its mRNA sequence is very similar to the canonical sequence except in two ways. TRPV1.var is missing the first exon found in the canonical sequence, so it starts with exon 2 as its exon 1. The greater difference between the canonical mRNA sequence and TRPV1.var is a retained intron found between exons 5 and 6. This 101 base pair intron introduces a frame shift error that truncates the protein to 253 amino acids. The forward primer used to isolate this variant was positioned to sit inside of the retained intron, and the reverse primer was situated further downstream and complements both the canonical and variant transcript.

Analysis of the first trial show that the sham-treatment group experienced a large increase in expression since its mean fold change value was 6.75±9.39, but due to its very large standard deviation, it cannot be said to be significantly different from either the control or CCI-treatment group. The CCI-treatment group showed virtually no change in expression relative to the control group, with a mean fold value of 1.2±1.1. The control group showed a greater than expected amount of variation between its members, with a mean fold value of 1.76±2.02. The mean fold value for the control group was generated

by comparing the control tissue samples to one another. In contrast, the second trial showed no real changes in expression between the three groups, as the difference between the three was no greater than 0.2 fold. Together, these data suggest that TRPV1.var expression is not affected by the CCI surgery. If anything, they suggest that the sham surgery had a greater effect on its expression. A reasonable explanation is that this variant is not expressed as highly in neurons than it is in renal tissue. This would make detection harder and less consistent between samples. A second related explanation could be that it is a variant that is not expressed uniformly between individuals. The authors that described TRPV1.var originally state that they were able to isolate its transcripts in multiple animals and from multiple tissue types, but they do not explicitly discuss how abundantly it is expressed [78].

In contrast to the studies of TRPV1 and its splice variants, the studies of NPY and Gap43, the positive control genes, generated data that did fit the predictions. There are a few explanations why the positive control studies worked and not TRPV1. The first explanation is that the primers designed for NPY and Gap43 work better. Unlike the primers for TRPV1, which all target parts of the mRNA toward the 5'-end, the primers for NPY and Gap43 target the 3'-end of the mRNA. This is a more reliable location for primers since it is less affected by problems during the reverse-transcription process, as mentioned before. The positive control primers are also more efficient since they can be positioned to target a region that will produce the least amount of unwanted primer-dimer products.

Pain assessment

A standard assessment of the efficacy of peripheral nerve injuries induced in murine animal models is to test for mechanical allodynia and thermal hyperalgesia of the plantar surface of the hind paws [92,95,107]. Unaffected animals generally do not react to the innocuous stimuli, and, if they do, it is generally to a relatively small degree. In contrast, injured animals will generally withdraw their paws faster from a radiant heat source, or in response to the pressure of a calibrated monofilament. Injured animals often will show physical changes that can be used as markers of the efficacy of pain models, including decreased weight, and altered gait.

This study shows that the CCI-treated rats, as a group, did display a slightly lowered threshold to pain, with respect to the mechanical pain assessment. The mean normalized withdrawal score for all animals was calculated by comparing the number of foot withdrawals for the left and right paws at day 8 and day 11. Neither time points, however, generated statistically significant results. At day 8, of the 8 CCI animals tested, only 2 displayed a lowered pain threshold; at day 11, of the 4 animals tested, only 2 displayed a lowered pain threshold. Only one CCI-treatment animal responded at both days, and no sham-treatment or control animal responded at either time point. Though only a trend, the data do support the time-dependent development of pain responses.

The thermal pain assessment data generated during this study cannot support the claim that the CCI-treatment animals had a significantly different mean withdrawal latency from either the sham-treatment or control group. As a tool for determining the effectiveness of the CCI treatment, measuring the withdrawal latency in response to a radiant heat source is a lot less reliable. It is a tool better served in the hands of an

experienced investigator since it can have more technical difficulties. For example, keeping the animals to remain in place for the duration of the testing can be challenging. The test requires that the animal have all 4 paws on the surface of the glass before the heat is turned on, and they must remain in contact during the entire testing. Rats, being rats, will investigate their surroundings and would often not remain stationary, interrupting the testing and forcing a restart. As mentioned previously, the rats would also protect their affected paw by keeping it raised or lying on their side to keep the paw off the ground. Occasionally, rats would stand on their rear paws to avoid the testing and to explore the Plexiglas chamber. Unlike during the mechanical testing, where the animals were contained in a wire cage, the rats were kept in a Plexiglas container on top of a glass plate. This resulted in their feces and urine affecting the testing by interfering with the sensor that would detect when a rat would lift its paw. As a consequence, I would have to stop the testing, remove the animal from the box, clean the surface, return the animal, and allow it to rehabituate. This increases the anxiety of already anxious animals, and may contribute to the large amount of variability of the mean normalized withdrawal scores.

Another technical difficulty of this study is the subjectivity of determining if a withdrawal is legitimate or not. The definition of a foot withdrawal is the full, voluntary removal of the paw from the testing surface in response to the stimuli being tested. The difficulty is determining, first, whether it is a legitimate withdrawal and not a shifting of weight or some other innocuous behavior, and second, whether or not the response is a result of the animal being in pain. A too stringent measurement would underreport the pain that the animals are experiencing, and a too lax measurement would inflate the pain

the animals experience; in this experiment, I believe it is more likely that I underreported legitimate withdrawals than over-reported.

The lack of pained behavior from 7 CCI-treatment animals on day 8, and the lack of pained behavior from 2 CCI-treatment animals on day 11 suggests that the surgery was not uniformly performed. Some animals may have had their sutures applied too tightly, resulting in a neuropathy instead of an inflamed sciatic nerve. Previous studies that have compared the results of different pain models have found that there are unique treatment dependent results. For example, a recent paper [108] found that crushing the sciatic nerve with forceps resulted in higher mechanical and thermal thresholds (meaning less pain was experienced), whereas an earlier paper showed that tightly ligating the sciatic nerve lowered mechanical and thermal thresholds slightly, but significantly [109]. Despite being fairly similar models, the entire sciatic nerve is damaged in both, very different results were achieved. Findings such as these reinforce how challenging it is to create reproducible pain models. However, both studies were in agreement that CCI, when properly performed, causes the greatest decrease in mechanical and thermal thresholds. Better surgeons will perform the CCI procedure consistently between animals, ensuring that each suture is properly tightened around the nerve. To further reinforce the point that proper induction of a neuropathic pain state is challenging, a paper from 2004 found that even the type of bedding an animal recovers in does have a significant effect on the development of pain [110].

A major limitation of this study is the population size of each group. There were only 4 animals for the CCI and Sham groups, and there were only 3 animals for the control group. Of the four CCI animals, only 2 showed signs of increased mechanical

allodynia, based on their difference scores. Assuming that the same rate of surgical success were achieved, if not better, than the mechanical and thermal data would likely become statistically significant.

Neuropeptide Y and Growth Associated Protein 43

The purpose of assaying Neuropeptide tyrosine (NPY) and Growth associated protein 43 (Gap43) expression was to provide additional molecular evidence that the sciatic nerve had been damaged following the CCI procedure. The increase of expression of both of these genes following peripheral nerve damage has been documented in a number of studies [87,100,101]. The results from from both trials demonstrate that NPY expression did significantly increase in level 5 DRGs ipsilateral to the CCI-treatment animals, in comparison to the sham-treatment and control. The increase in expression of Gap43 was statistically significant in the first trial but not the second trial. The value of these data is that they demonstrate that there are statistically significant treatment-dependent effects following CCI.

Within the pain transduction pathway, NPY is believed to have an anti-nociceptive and anti-allodynic effect. It is a neuropeptide that is released by DRG neurons into the central terminal, where it then binds to its receptors (Y1 and Y2) in the substantia gelatinosa [85]. The activation of Y1 and Y2 is believed to inhibit painful signals multiple ways. One way is that Y2 activation causes the the release of glutamate from spinal synaptosomes to be attenuated. A second way is that after peripheral nerve damage, Y2 activation reduces Ca^{++} channel conductance [85]. If NPY is upregulated following peripheral nerve damage, then Y1 and Y2 receptors will be activated more, further reduce channel conductance, and diminish pain signals to the brain. This was

further demonstrated with $Y1^{-/-}$ mice [66,111]. These mice showed reduced latencies in the hot plate test, and showed greater allodynia following injection of complete Freund's adjuvant into their hind paws. Additionally, intrathecal injection of NPY did not diminish the nociception in these mice, whereas it normally does in wildtype mice [111]. The increase in NPY in DRG neurons in this study, therefore, can be used as additional evidence that the animals likely experienced allodynia and hyperalgesia, even though the behavioral data does not bear it out. Gap43 is a protein found primarily in the cytoskeleton and plasma membrane. It is a highly expressed growth-associated protein that plays a key role in axon guidance and connection formation during the development of the vertebrate nervous system [112,113]. In the mature nervous system, Gap43 expression is much lower. Following peripheral nerve damage, the expression of Gap43 is upregulated and is associated with axonal regeneration [114,115]. Therefore, its differential expression can be used as measure of peripheral nerve damage. The results in this study are consistent with the published literature and demonstrate that increased Gap43 expression is indicative of neuronal trauma occurring only in the CCI-treated animals. Gap43 has not been shown to be involved in the pain transduction, so its upregulation cannot be associated with the onset of neuropathic pain, however. Likewise, neither of these genes can be used to demonstrate that the neuronal trauma experienced by these rats reflects the symptoms experienced during Complex Regional Pain Syndrome II.

Mirror pain

One interesting piece of data that emerged from this study is the increased expression of TRPV1 in the contralateral (left) side of the CCI-treatment animals in the

1-step analysis. A comparison of the ipsilateral versus contralateral fold changes revealed that there was no significant difference in expression between the sides. Additionally, the mean ΔCt values for the left and right sides were very close (Ipsilateral = 3.15, Contralateral = 2.70), and both were lower than either the control or sham-treatment animals.

Mirror pain is a phenomenon that occurs in chronic pain conditions where pain is experienced on the side contralateral to the original injury [95]. Mirror pain is also responsible for allodynia in the contralateral side, so otherwise innocuous stimuli become uncomfortable and painful. Presently, its origin has yet to be determined, although several mechanisms have been proposed. These include the alteration of neurocircuits, which changes how sensory information is processed [98,116]. Milligan et al. [98] found in their study that the severity of mirror pain experienced by Sprague-Dawley rats is correlated with the level of immune activation caused by perisciatic microinjections of yeast cell walls. Lower doses of the activator cause unilateral inflammation, and larger doses induce bilateral allodynia. They also found that they could inhibit mirror pain with the intrathecal administration of proinflammatory antagonists, such as TNFbp. They are unsure of how it is initiated, but they believe that the strong activation of proinflammatory molecules is able to activate glial cells in one side of the dorsal horn, and then propagate across to the other side via gap junctions and slow calcium waves.

Kleinschnitz et al. [117] reported similar data to that of Milligan et al. [98]. They found that CCI increased the mRNA expression of certain cytokines and chemokines in an NMDA receptor dependent manner. Specifically, they were able to show that CCI

increases the mRNA expression of Interleukin-1β, Interleukin-10, and monocyte chemoattractant protein-1 in the contralateral DRG.

An earlier study by Oaklander and Belzberg [118] found that the unilateral nerve transection of the sciatic nerve distal to the DRG downregulates the sodium channel *SCN10A* bilaterally in rat DRGs. The significance of this report is that spontaneous action potentials arising from the dorsal horn ipsilateral to the nerve injury may increase mechanosensitivity in the contralateral dorsal horn, causing mirror pain. Previous reports that they cite found that sciatic nerve transection increases the mRNA encoding for a different sodium channel subtype, *SCN3A*. A change in the subtypes composing sodium channels in the dorsal horn, following nerve injury, may contribute to the generation of mirror pain.

Within the context of these other papers, the fact that TRPV1 mRNA expression increased in the contralateral (left) DRG seems less surprising. The increase in expression would suggest that the animals may have experienced mirror pain, but without the corroborating behavioral data, the claim remains speculative. Either way, the data presented here does support the claim that unilateral nerve injuries can affect the transcription of genes in the contralateral DRGs.

Power analysis of real-time data

Because this study relied on a small sample size for each treatment group, it was thought that the power of this study might be below the commonly accepted power level of 80%. To test this, a post-hoc power analysis was performed on the data generated from the TRPV1 real-time experiment using RNA as the template material. The results of the power analysis found that the study, in fact, did not have enough animals in each

treatment group to achieve 80% power. A minimum of 6 animals in each treatment group would be required to conclude with full confidence that a p-value of 0.087 is not statistically significant. As a result, it cannot be definitively ruled that CCI does not alter the expression of TRPV1. It still must be accepted, however, that the mean TRPV1 expression of the CCI-treatment group is not significantly different from TRPV1 expression in the sham-treatment or control groups. The results of this power-analysis also cannot be used to claim that the CCI procedure will generate statistically significant results if a minimum of 18 animals are used.

Ankyrin repeats and the effects of alternative splicing within TRPV1

With the exception of TRPV1.var, which has a small 11 base pair deletion in the C-terminal region and TRPV1.son, which is a C-terminal fragment of TRPV1, the rest of the known splice events occur in the N-terminal cytosolic region. Within the N-terminal region, the largest feature is the ankyrin repeat domain (ARD). Initial analysis of the protein predicted there to be 3 ankyrin repeats [35] in the N-terminal region, but a 2007 paper by Lishko et al. [39] demonstrated via crystallography that there are actually 6 ankyrin repeats in TRPV1. The discrepancy between the two papers may be explained by the fact that older methods of detecting the terminal ankyrin repeats in a domain had difficulty due evolutionary divergences between species [119]. The analysis by Lishko et al. determined that the ARD encompasses amino acids 101 through 364, and is encoded by exons 2 through 7. Exon 7 only codes for the final 17 amino acids of the ARD, which means that the splice variant TRPV1.β does not affect the domain. Other splice variants, such as TRPV1.5'sv, TRPV1.var, and TRPV1.b, do have splicing events that occurs within the ARD. The variant TRPV1.5'sv has the greatest amount of splicing occurring

in the ARD since it starts with exon 5 and is missing the entire seventh exon. See Figure 22 for a cartoon comparing the different N-terminal regions of TRPV1 and its splice variants.

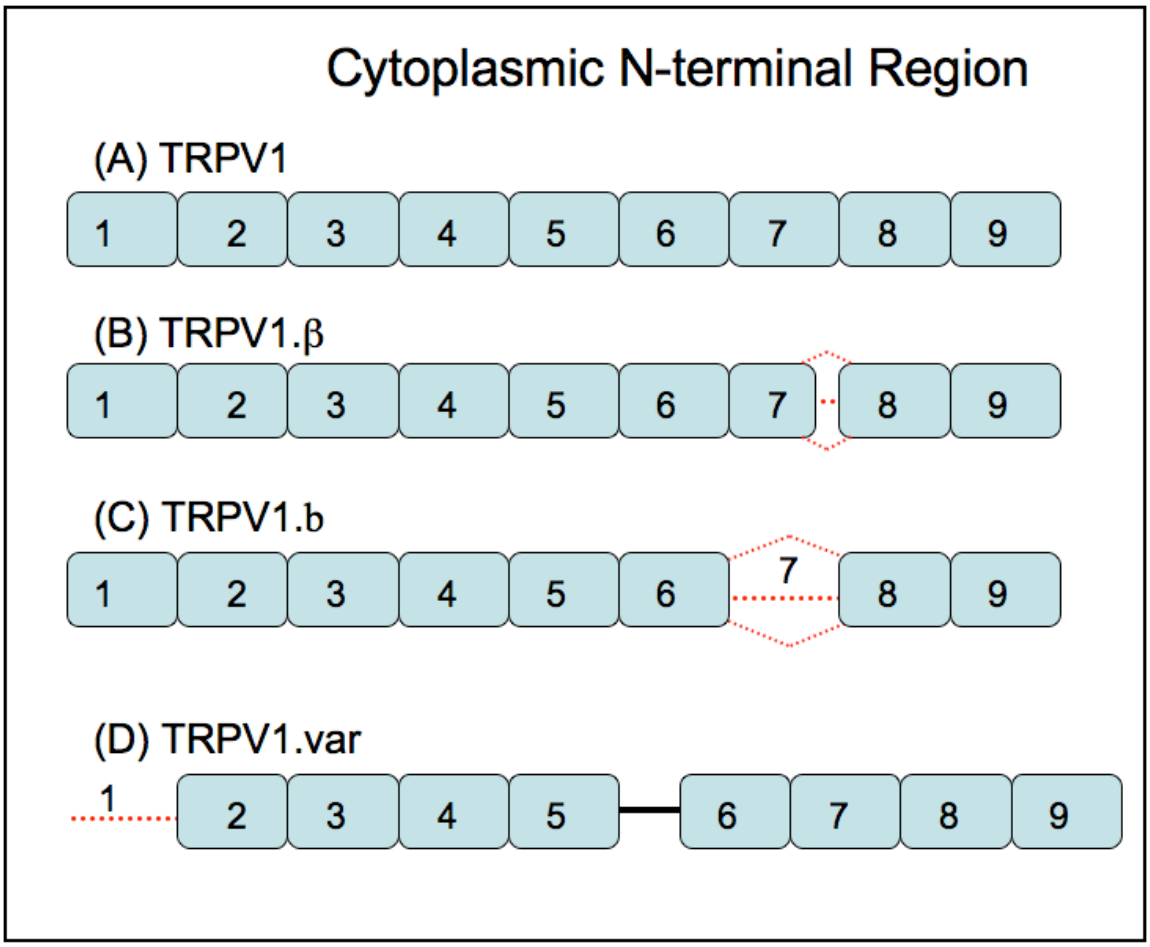

Figure 22. Comparison of the Cytoplasmic N-Terminal Regions of TRPV1 and its Splice Variants

(A) Shown here is the canonical cytoplasmic N-terminal of TRPV1, which is coded for by exons 1-8
(B) Shown here is the spliced version of TRPV1.β. 10 amino acids are removed from the end of exon 7. Red dotted lines indicate spliced out segment.
(C) Shown here is the spliced version of TRPV1.b. The entire seventh exon is missing
(D) Shown here is the spliced version of TRPV1.var. It utilizes an alternative transcriptional start site that skips exon 1 and it retains an intron between exons 5 and 6. Solid black line indicates retained intron.

Ankyrin repeats are one of the most common amino acid motifs found in proteins. They were first characterized in yeast cell cycle regulatory proteins, and given the name ankyrin after the cytoskeletal protein, which has 24 of the repeats [120]. Ankyrin repeats are involved a variety of cellular functions, but are most commonly associated with protein-protein interaction. In TRPV5 and TRPV6, the ARD has been shown to be necessary for functional channel assembly [121]. Lishko et al. showed that for TRPV1 the role for the ARD is not involved in channel assembly, but actually channel modulation [39].

They showed that the ARD is involved with channel modulation based on how the binding of calmodulin and ATP have opposing effects on the channel. During normal conditions, TRPV1 is in a sensitized state and will react to ligands or stimuli. Following repeated stimulation, such as by repeated capsaicin applications, TRPV1 enters into a tachyphylactic state wherein it is resistant to further stimulation and will not open. During this desensitized state, it has been recognized that people experiencing pain find some relief. The reason that they feel relief following the repeated capsaicin application is that calmodulin (CaM) binds to the ARD of TRPV1 and prevents the channel from opening. The binding of CaM is Ca^{++} dependent and only occurs after TRPV1 opens up and allows for an influx of Ca^{++} ions. As the Ca^{++} ions are re-sequestered, CaM is replaced by ATP, which returns the TRPV1 channel to a sensitized state. The shared binding site for ATP and CaM is spread between the first three ankyrin repeats and involves 7 key residues. Exons 2-4 code for these residues and are not affected by splicing events to form TRPV1.β, TRPV1.b, and TRPV1.var, but are affected by the

splicing necessary to form TRPV1.5'sv. TRPV1.5'sv is missing the first 4 exons, and therefore lacks the ATP/CaM binding site.

Other known proteins that interact with the TRPV1 ARD include a variety of different kinases, including Protein Kinase A (PKA), Protein Tyrosine Kinase (PTK), and SRC Kinase [122,123]. These kinases mediate the effects of many of the intracellular molecules that sensitize TRPV1. Therefore, the removal of phosphorylation sites could prevent the sensitization of TRPV1 to intracellular signaling molecules. That might prevent or diminish the hyperalgesia or allodynia experienced by following TRPV1 sensitization. In terms of the splice variants studied in this project, only one residue in exon 7 is targeted by PKA: Tyrosine 370, and it is only removed in the formation of TRPV1.b. The variant TRPV1.var has no transmembrane domain, so it would not be affected by the kinases. The authors that described TRPV1.var suggest that it could be a decoy molecule for intermediate signaling molecules, allowing the canonical forms to go unaltered. Though they do not explain how or where, the authors also suggest that TRPV1.var may interfere with proper channel architecture [78]. With regard to TRPV1.β, only 10 amino acids are missing from the end of exon 7. Despite being a relatively small deletion, the loss of those 10 residues causes the protein to become quite unstable. The deletion occurs in the region between the ARD and the transmembrane domain. Only a small proportion of TRPV1.β proteins manage to make it into the plasma membrane. Once inserted into channels, TRPV1.β causes the channel to become insensitive to capsaicin or protons. This is an odd finding since the capsaicin binding site is located in the transmembrane domains, and the proton binding sites are extracellular. The authors conclude that TRPV1.β has a dominant-negative effect, and that its

upregulation may be a way to desensitize capsaicin sensitive cells without causing cellular death [71].

In contrast to TRPV1.β, and its 10 amino acid deletion, TRPV1.b is missing the entire exon 7 and is able to form functional ion channels that are temperature sensitive but not capsaicin or proton sensitive [70]. The authors make the argument that during times of inflammation, channels that have TRPV1.b as a subunit, or are made entirely of TRPV1.b, would only act as thermal transducers, potentially diminishing painful signals. Their hypothesis, however, seems to be contradicted by Charrua et al. [83] who found that TRPV1.b expression is downregulated in a cystitis rat model. Charrua et al. seem to suggest that during non-painful conditions TRPV1.b keeps the TPRV1 channel from being too sensitive to capsaicin or protons, and during painful conditions TRPV1.b causes the TRPV1 channel to become more sensitive through its downregulation. While not statistically significant, the trend of increased expression would support Lu et al., and their hypothesis that TRPV1.b helps to desensitize TRPV1 channels.

The original paper by Lu et al. [70] describing TRPV1.b, suggests that only a small population of cells within the DRG express the variant. These nociceptors may be responsible for only responding to temperatures even higher than the canonical TRPV1 protein. How the removal of exon 7 effects this change is not clear from the paper, but it does say that this isoform is no longer responsive to protons or to capsaicin. The suggestion is that the lack of exon 7 is affecting how capsaicin binds to its receptor site, which is located between transmembrane 2 and 3.

Immunohistochemical and confocal microscopy data

The result of the immunohistochemical data are that TRPV1 expression is increased in a subset of DRG neurons that innervate the plantar surface of the right rear paw of rats following CCI surgery. We were able to demonstrate this through the use of a fluorescent retrograde neuronal tracer and fluorescent antibodies specific for TRPV1 and Neurofilament-M, a protein expressed only in neuronal cells. We showed that relative fluorescent intensity of TRPV1 expression relative to DiD expression was greater in CCI affected DRGs compared to DRGs from control animals.

As previously mentioned, TRPV1 is expressed primarily in neurons with medium-to-small, myelinated Aδ fibers and small neurons with unmyelinated C-fibers. What can be seen in Figure 23 is that TRPV1 is primarily being expressed in medium (500-1000μm^2) sized neurons. Neurons of this size are typically associated with Aδ delta fibers. This is consistent with what is reported in the literature [124, 125]. In some studies, the expression of TRPV1 and other TRP proteins has increased in large neurons, but that was not documented here. A study by Staaf et al. (2009) demonstrated that TRPML3, for example, was upregulated in larger diameter DRG neurons following the spared nerve injury [87]. Large neurons are normally associated with innocuous sensation, not nociception, but it is believed that they can be recruited into expressing TRPV1 during chronic pain states [87].

Chapter 5

FUTURE WORK

Replication using larger sample sizes

The lack of power in this study prevented us from demonstrating that there are significant differences in TRPV1 expression between the three different groups. We lacked the necessary power because our sample size was to small to compensate for some of the surgical deficits we encountered. We would like to replicate this study using the necessary animals to achieve statistical significance. The preliminary data we generated from the immunohistochemical data was also intriguing, and we want to pursue that as well. It would be interesting to see if we could generate isoform specific antibodies for this work. We would also like to replicate the study primarily using direct from mRNA amplification.

Analysis of other TRP genes and their splice variants

Splice variants have been isolated in many other TRP genes, including TRPV4, TRPM8, and TRPC1, among others [126]. TRPV4 and TRPM8 are both ThermoTRPs, just like TRPV1, so characterizing the contribution of their splice variants to the generation and maintenance of neuropathic pain conditions would further increase our ability to treat pain. A TRP that has no known current splice variants is TRPA1. It and TRPM8 are believed to be the primary detectors of cold, menthol, and mustard oil [27]. Both it and TRPM8 are known to be upregulated in response to the CCI procedure. We

would like to perform studies to determine if TRPA1 has splice variants, and what their contribution to neuropathic pain would be.

Cell culturing of primary neurons or cell lines

As described above, one of the greatest difficulties of this kind of research is attaining adequate sample sizes to generate robust, significant data. A reasonable alternative might be culturing primary neurons obtained from DRGs, or using immortalized rat neuronal cell lines instead of live animals. The advantages of utilizing cell lines include infinite sample sizes, greater schedule flexibility, and unlimited amounts of RNA. Additionally, using these cell cultures would be more humane, and in line with the idea of using fewer animals to generate comparable data. The greatest disadvantage to this approach is that no behavioral data can be generated. The other real challenge would be determining if the cells can be properly stimulated by pro-inflammatory molecules to induce a differential expression of TRPV1. The CCI method is intended to barely impinge the sciatic nerve, and create an inflammation around the sutures, so if the cells could be directly stimulated with pro-inflammatory molecules, there would be less reason to perform the surgeries and use rats.

Some work in this area has already been done. One of the first studies to demonstrate the Nerve Growth Factor (NGF) directly affects TRPV1 expression was done using cultured DRG neurons. Winston et al. (2001) [127] showed that TRPV1 expression in cultures of adult rat DRG neurons increase in a NGF dose-dependent manner. They measured the increase of TRPV1 in two ways. The first way they measured NGF's effect on TRPV1 expression was by measuring the release of calcitonin gene related peptide (CGRP) from DRG neurons. Previous reports had shown that

capsaicin causes the depolarization of neurons and the release of CGRP. The application of NGF in a dose-dependent manner resulted in the increase of TRPV1 channels that could be activated by capsaicin, allowing for a greater release of CGRP. The second way they showed that NGF increases the expression was by using Northern blots to directly measuring the TRPV1 mRNA levels following NGF application. Other similarly designed studies have been conducted to show that TRPV1 expression can be regulated by other intracellular pathways. For example, a recent paper showed that administration of alpha 2-adrenoreceptor agonists can attenuate capsaicin-evoked substance P (an inflammatory molecule) release in cultured DRG neurons [128].

Cultures of DRG neurons can also be used to study TRPV1 splice variants. The same paper that showed that TRPV1.b overexpression attenuates the sensitivity of TRPV1 to capsaicin, also showed that TRPV1.b can be isolated and analyzed in DRG cultures. The role that splice variants play when inflammation or peripheral nerve damage has occurred is only beginning to be studied. Using DRG cultures would allow scientists to more easily tease out what effects individual inflammatory molecules have on splice variant expression in vivo. We know that NGF increases TRPV1 expression, but it is currently unknown if it has the same effect on its splice variants.

REFERENCES

1 in *Classification of Chronic Pain: Descriptions of Chronic Pain Syndromes and Definitions of Pain Terms, Second Edition* (ed Harold Merskey, Bogduk, Nikolai) 209-213 (IASP Press, 1994).

2 *Pain: Hope Through Research*, <http://www.ninds.nih.gov/disorders/chronic_pain/detail_chronic_pain.htm> (2001).

3 (ed American Pain Foundation) (Baltimore, 2009).

4 Stewart, W. F., Ricci, J. A., Chee, E., Morganstein, D. & Lipton, R. Lost productive time and cost due to common pain conditions in the US workforce. *JAMA* **290**, 2443-2454, doi:10.1001/jama.290.18.2443 290/18/2443 [pii] (2003).

5 Weiner, K. 1-3 (American Academy of Pain Management).

6 (ed The U.S. Food and Drug Administration) (2007).

7 Strassels, S. A. Economic burden of prescription opioid misuse and abuse. *J Manag Care Pharm* **15**, 556-562, doi:2009(15)7: 556-562 [pii] (2009).

8 Argoff, C. E. & Silvershein, D. I. A comparison of long- and short-acting opioids for the treatment of chronic noncancer pain: tailoring therapy to meet patient needs. *Mayo Clin Proc* **84**, 602-612, doi:84/7/602 [pii] 10.4065/84.7.602 (2009).

9 Coluzzi, F. & Pappagallo, M. Opioid therapy for chronic noncancer pain: practice guidelines for initiation and maintenance of therapy. *Minerva Anestesiol* **71**, 425-433 (2005).

10 Levine, J. D. & Alessandri-Haber, N. TRP channels: targets for the relief of pain. *Biochim Biophys Acta* **1772**, 989-1003, doi:S0925-4439(07)00032-4 [pii] 10.1016/j.bbadis.2007.01.008 (2007).

11 (The MayDay Fund, 2009).

12 Sherrington, C. S. Qualitative differences of spinal reflex corresponding with qualitative difference of cutaneous stimulus. *J Physiol* **30**, 39-46 (1903).

13 Sherrington, C. S. *The integrative action of the nervous system*. (Scribner, 1906).

14 Woolf, C. J. & Ma, Q. Nociceptors--noxious stimulus detectors. *Neuron* **55**, 353-364, doi:S0896-6273(07)00537-5 [pii] 10.1016/j.neuron.2007.07.016 (2007).

15 Craig, A. D. & Sorkin, L. S. (John Wiley & Sons, Ltd., 2005).

16 Hotta, Y. & Benzer, S. Abnormal electroretinograms in visual mutants of Drosophila. *Nature* **222**, 354-356 (1969).

17 Montell, C. & Rubin, G. M. Molecular characterization of the Drosophila trp locus: a putative integral membrane protein required for phototransduction. *Neuron* **2**, 1313-1323, doi:0896-6273(89)90069-X [pii] (1989).

18 Montell, C. *et al.* A unified nomenclature for the superfamily of TRP cation channels. *Mol Cell* **9**, 229-231, doi:S1097276502004483 [pii] (2002).

[19] Nilius, B., Owsianik, G., Voets, T. & Peters, J. A. Transient receptor potential cation channels in disease. *Physiol Rev* **87**, 165-217, doi:87/1/165 [pii] 10.1152/physrev.00021.2006 (2007).

[20] Xu, X. Z., Moebius, F., Gill, D. L. & Montell, C. Regulation of melastatin, a TRP-related protein, through interaction with a cytoplasmic isoform. *Proc Natl Acad Sci U S A* **98**, 10692-10697, doi:10.1073/pnas.191360198 191360198 [pii] (2001).

[21] Bassi, M. T. *et al.* Cloning of the gene encoding a novel integral membrane protein, mucolipidin-and identification of the two major founder mutations causing mucolipidosis type IV. *Am J Hum Genet* **67**, 1110-1120, doi:S0002-9297(07)62941-3 [pii] 10.1016/S0002-9297(07)62941-3 (2000).

[22] Sun, M. *et al.* Mucolipidosis type IV is caused by mutations in a gene encoding a novel transient receptor potential channel. *Hum Mol Genet* **9**, 2471-2478 (2000).

[23] Story, G. M. *et al.* ANKTM1, a TRP-like channel expressed in nociceptive neurons, is activated by cold temperatures. *Cell* **112**, 819-829, doi:S0092867403001582 [pii] (2003).

[24] Torres, V. E. & Harris, P. C. Autosomal dominant polycystic kidney disease: the last 3 years. *Kidney Int* **76**, 149-168, doi:ki2009128 [pii] 10.1038/ki.2009.128 (2009).

[25] Voets, T., Talavera, K., Owsianik, G. & Nilius, B. Sensing with TRP channels. *Nat Chem Biol* **1**, 85-92, doi:nchembio0705-85 [pii] 10.1038/nchembio0705-85 (2005).

[26] Huang, C. L. The transient receptor potential superfamily of ion channels. *J Am Soc Nephrol* **15**, 1690-1699 (2004).

[27] Venkatachalam, K. & Montell, C. TRP channels. *Annu Rev Biochem* **76**, 387-417, doi:10.1146/annurev.biochem.75.103004.142819 (2007).

[28] Cuypers, E., Yanagihara, A., Karlsson, E. & Tytgat, J. Jellyfish and other cnidarian envenomations cause pain by affecting TRPV1 channels. *FEBS Lett* **580**, 5728-5732, doi:S0014-5793(06)01118-5 [pii] 10.1016/j.febslet.2006.09.030 (2006).

[29] Liedtke, W. & Friedman, J. M. Abnormal osmotic regulation in trpv4-/- mice. *Proc Natl Acad Sci U S A* **100**, 13698-13703, doi:10.1073/pnas.1735416100 1735416100 [pii] (2003).

[30] Peier, A. M. *et al.* A TRP channel that senses cold stimuli and menthol. *Cell* **108**, 705-715, doi:S0092867402006529 [pii] (2002).

[31] Zhang, Y. *et al.* Coding of sweet, bitter, and umami tastes: different receptor cells sharing similar signaling pathways. *Cell* **112**, 293-301, doi:S0092867403000710 [pii] (2003).

[32] Inoue, R. TRP channels as a newly emerging non-voltage-gated CA2+ entry channel superfamily. *Curr Pharm Des* **11**, 1899-1914 (2005).

[33] Rutter, A. R., Ma, Q. P., Leveridge, M. & Bonnert, T. P. Heteromerization and colocalization of TrpV1 and TrpV2 in mammalian cell lines and rat dorsal root ganglia. *Neuroreport* **16**, 1735-1739, doi:00001756-200511070-00003 [pii] (2005).

[34] Bandell, M., Macpherson, L. J. & Patapoutian, A. From chills to chilis: mechanisms for thermosensation and chemesthesis via thermoTRPs. *Curr Opin Neurobiol* **17**, 490-497, doi:S0959-4388(07)00097-9 [pii] 10.1016/j.conb.2007.07.014 (2007).

[35] Caterina, M. J. *et al.* The capsaicin receptor: a heat-activated ion channel in the pain pathway. *Nature* **389**, 816-824, doi:10.1038/39807 (1997).

[36] Siemens, J. *et al.* Spider toxins activate the capsaicin receptor to produce inflammatory pain. *Nature* **444**, 208-212, doi:nature05285 [pii] 10.1038/nature05285 (2006).

[37] Macpherson, L. J. *et al.* The pungency of garlic: activation of TRPA1 and TRPV1 in response to allicin. *Curr Biol* **15**, 929-934, doi:S0960-9822(05)00391-X [pii] 10.1016/j.cub.2005.04.018 (2005).

[38] Woo, D. H. *et al.* Direct activation of transient receptor potential vanilloid 1(TRPV1) by diacylglycerol (DAG). *Mol Pain* **4**, 42, doi:1744-8069-4-42 [pii] 10.1186/1744-8069-4-42 (2008).

[39] Lishko, P. V., Procko, E., Jin, X., Phelps, C. B. & Gaudet, R. The ankyrin repeats of TRPV1 bind multiple ligands and modulate channel sensitivity. *Neuron* **54**, 905-918, doi:S0896-6273(07)00406-0 [pii] 10.1016/j.neuron.2007.05.027 (2007).

[40] Anand, U. *et al.* The effect of neurotrophic factors on morphology, TRPV1 expression and capsaicin responses of cultured human DRG sensory neurons. *Neurosci Lett* **399**, 51-56, doi:S0304-3940(06)00078-4 [pii] 10.1016/j.neulet.2006.01.046 (2006).

[41] Moriyama, T. *et al.* Sensitization of TRPV1 by EP1 and IP reveals peripheral nociceptive mechanism of prostaglandins. *Mol Pain* **1**, 3, doi:1744-8069-1-3 [pii] 10.1186/1744-8069-1-3 (2005).

[42] Szallasi, A., Cortright, D. N., Blum, C. A. & Eid, S. R. The vanilloid receptor TRPV1: 10 years from channel cloning to antagonist proof-of-concept. *Nat Rev Drug Discov* **6**, 357-372, doi:nrd2280 [pii] 10.1038/nrd2280 (2007).

[43] Vennekens, R., Owsianik, G. & Nilius, B. Vanilloid transient receptor potential cation channels: an overview. *Curr Pharm Des* **14**, 18-31 (2008).

[44] Holzer, P. Local effector functions of capsaicin-sensitive sensory nerve endings: involvement of tachykinins, calcitonin gene-related peptide and other neuropeptides. *Neuroscience* **24**, 739-768 (1988).

[45] Tominaga, M. *et al.* The cloned capsaicin receptor integrates multiple pain-producing stimuli. *Neuron* **21**, 531-543, doi:S0896-6273(00)80564-4 [pii] (1998).

[46] Charrua, A. *et al.* Functional transient receptor potential vanilloid 1 is expressed in human urothelial cells. *J Urol* **182**, 2944-2950, doi:S0022-5347(09)02018-7 [pii] 10.1016/j.juro.2009.08.022 (2009).

[47] Avelino, A. & Cruz, F. TRPV1 (vanilloid receptor) in the urinary tract: expression, function and clinical applications. *Naunyn Schmiedebergs Arch Pharmacol* **373**, 287-299, doi:10.1007/s00210-006-0073-2 (2006).

[48] Inoue, R. *et al.* Transient receptor potential channels in cardiovascular function and disease. *Circ Res* **99**, 119-131, doi:99/2/119 [pii]

10.1161/01.RES.0000233356.10630.8a (2006).
49 Inoue, R., Jian, Z. & Kawarabayashi, Y. Mechanosensitive TRP channels in cardiovascular pathophysiology. *Pharmacol Ther* **123**, 371-385, doi:S0163-7258(09)00113-2 [pii]
10.1016/j.pharmthera.2009.05.009 (2009).
50 Mezey, E. *et al.* Distribution of mRNA for vanilloid receptor subtype 1 (VR1), and VR1-like immunoreactivity, in the central nervous system of the rat and human. *Proc Natl Acad Sci U S A* **97**, 3655-3660, doi:10.1073/pnas.060496197 060496197 [pii] (2000).
51 Cui, M. *et al.* TRPV1 receptors in the CNS play a key role in broad-spectrum analgesia of TRPV1 antagonists. *J Neurosci* **26**, 9385-9393, doi:26/37/9385 [pii] 10.1523/JNEUROSCI.1246-06.2006 (2006).
52 Sanchez, J. F., Krause, J. E. & Cortright, D. N. The distribution and regulation of vanilloid receptor VR1 and VR1 5' splice variant RNA expression in rat. *Neuroscience* **107**, 373-381, doi:S0306-4522(01)00373-6 [pii] (2001).
53 LaMotte, R. H., Lundberg, L. E. & Torebjork, H. E. Pain, hyperalgesia and activity in nociceptive C units in humans after intradermal injection of capsaicin. *J Physiol* **448**, 749-764 (1992).
54 Gilchrist, H. D., Allard, B. L. & Simone, D. A. Enhanced withdrawal responses to heat and mechanical stimuli following intraplantar injection of capsaicin in rats. *Pain* **67**, 179-188, doi:0304-3959(96)03104-1 [pii] (1996).
55 Hong, S., Agresta, L., Guo, C. & Wiley, J. W. The TRPV1 receptor is associated with preferential stress in large dorsal root ganglion neurons in early diabetic sensory neuropathy. *J Neurochem* **105**, 1212-1222, doi:JNC5220 [pii] 10.1111/j.1471-4159.2008.05220.x (2008).
56 Xu, G. Y. *et al.* Transient receptor potential vanilloid 1 mediates hyperalgesia and is up-regulated in rats with chronic pancreatitis. *Gastroenterology* **133**, 1282-1292, doi:S0016-5085(07)01156-0 [pii]
10.1053/j.gastro.2007.06.015 (2007).
57 Niiyama, Y., Kawamata, T., Yamamoto, J., Omote, K. & Namiki, A. Bone cancer increases transient receptor potential vanilloid subfamily 1 expression within distinct subpopulations of dorsal root ganglion neurons. *Neuroscience* **148**, 560-572, doi:S0306-4522(07)00664-1 [pii]
10.1016/j.neuroscience.2007.05.049 (2007).
58 Szabo, A. *et al.* Role of transient receptor potential vanilloid 1 receptors in adjuvant-induced chronic arthritis: in vivo study using gene-deficient mice. *J Pharmacol Exp Ther* **314**, 111-119, doi:jpet.104.082487 [pii]
10.1124/jpet.104.082487 (2005).
59 Jones, R. C., 3rd, Xu, L. & Gebhart, G. F. The mechanosensitivity of mouse colon afferent fibers and their sensitization by inflammatory mediators require transient receptor potential vanilloid 1 and acid-sensing ion channel 3. *J Neurosci* **25**, 10981-10989, doi:25/47/10981 [pii]
10.1523/JNEUROSCI.0703-05.2005 (2005).
60 Caterina, M. J. *et al.* Impaired nociception and pain sensation in mice lacking the capsaicin receptor. *Science* **288**, 306-313, doi:8443 [pii] (2000).

[61] Bolcskei, K. *et al.* Investigation of the role of TRPV1 receptors in acute and chronic nociceptive processes using gene-deficient mice. *Pain* **117**, 368-376, doi:S0304-3959(05)00325-8 [pii] 10.1016/j.pain.2005.06.024 (2005).

[62] Hudson, L. J. *et al.* VR1 protein expression increases in undamaged DRG neurons after partial nerve injury. *Eur J Neurosci* **13**, 2105-2114, doi:ejn1591 [pii] (2001).

[63] Kanai, Y., Nakazato, E., Fujiuchi, A., Hara, T. & Imai, A. Involvement of an increased spinal TRPV1 sensitization through its up-regulation in mechanical allodynia of CCI rats. *Neuropharmacology* **49**, 977-984, doi:S0028-3908(05)00186-3 [pii] 10.1016/j.neuropharm.2005.05.003 (2005).

[64] Kasama, S. *et al.* RNA interference-mediated knock-down of transient receptor potential vanilloid 1 prevents forepaw inflammatory hyperalgesia in rat. *Eur J Neurosci* **25**, 2956-2963, doi:EJN5584 [pii] 10.1111/j.1460-9568.2007.05584.x (2007).

[65] Fukuoka, T. *et al.* VR1, but not P2X(3), increases in the spared L4 DRG in rats with L5 spinal nerve ligation. *Pain* **99**, 111-120, doi:S0304395902000672 [pii] (2002).

[66] Zeyzus, B. *TRPV1 MRNA IS DIFFERENTIALLY EXPRESSED IN DIFFERENT VERTEBRAL LEVELS OF RAT DORSAL ROOT GANGLIA FOLLOWING SCIATIC NERVE INJURY* Masters of Biology thesis, Duquesne University, (2009).

[67] Black, D. L. Mechanisms of alternative pre-messenger RNA splicing. *Annu Rev Biochem* **72**, 291-336, doi:10.1146/annurev.biochem.72.121801.161720 121801.161720 [pii] (2003).

[68] Tolnay, M. & Probst, A. REVIEW: tau protein pathology in Alzheimer's disease and related disorders. *Neuropathol Appl Neurobiol* **25**, 171-187, doi:nan182 [pii] (1999).

[69] Magen, A. & Ast, G. The importance of being divisible by three in alternative splicing. *Nucleic Acids Res* **33**, 5574-5582, doi:33/17/5574 [pii] 10.1093/nar/gki858 (2005).

[70] Lu, G., Henderson, D., Liu, L., Reinhart, P. H. & Simon, S. A. TRPV1b, a functional human vanilloid receptor splice variant. *Mol Pharmacol* **67**, 1119-1127, doi:mol.104.009852 [pii] 10.1124/mol.104.009852 (2005).

[71] Wang, C., Hu, H. Z., Colton, C. K., Wood, J. D. & Zhu, M. X. An alternative splicing product of the murine trpv1 gene dominant negatively modulates the activity of TRPV1 channels. *J Biol Chem* **279**, 37423-37430, doi:10.1074/jbc.M407205200 M407205200 [pii] (2004).

[72] Lyall, V. *et al.* A novel vanilloid receptor-1 (VR-1) variant mammalian salt taste receptor. *Chem Senses* **30 Suppl 1**, i42-43, doi:30/suppl_1/i42 [pii] 10.1093/chemse/bjh104 (2005).

[73] Valadkhan, S. The spliceosome: caught in a web of shifting interactions. *Curr Opin Struct Biol* **17**, 310-315, doi:S0959-440X(07)00065-6 [pii] 10.1016/j.sbi.2007.05.001 (2007).

[74] Wahl, M. C., Will, C. L. & Luhrmann, R. The spliceosome: design principles of a dynamic RNP machine. *Cell* **136**, 701-718, doi:S0092-8674(09)00146-9 [pii] 10.1016/j.cell.2009.02.009 (2009).

[75] Li, Q., Lee, J. A. & Black, D. L. Neuronal regulation of alternative pre-mRNA splicing. *Nat Rev Neurosci* **8**, 819-831, doi:nrn2237 [pii] 10.1038/nrn2237 (2007).

[76] Nilsen, T. W. & Graveley, B. R. Expansion of the eukaryotic proteome by alternative splicing. *Nature* **463**, 457-463, doi:nature08909 [pii] 10.1038/nature08909.

[77] Valcarcel, J. & Smith, C. W. J. (John Wiley & Sons, Ltd., 2005).

[78] Tian, W., Fu, Y., Wang, D. H. & Cohen, D. M. Regulation of TRPV1 by a novel renally expressed rat TRPV1 splice variant. *Am J Physiol Renal Physiol* **290**, F117-126, doi:00143.2005 [pii] 10.1152/ajprenal.00143.2005 (2006).

[79] Schumacher, M. A., Moff, I., Sudanagunta, S. P. & Levine, J. D. Molecular cloning of an N-terminal splice variant of the capsaicin receptor. Loss of N-terminal domain suggests functional divergence among capsaicin receptor subtypes. *J Biol Chem* **275**, 2756-2762 (2000).

[80] Schumacher, M. A. *et al.* The stretch-inactivated channel, a vanilloid receptor variant, is expressed in small-diameter sensory neurons in the rat. *Neurosci Lett* **287**, 215-218, doi:S0304394000011812 [pii] (2000).

[81] Sharif Naeini, R., Witty, M. F., Seguela, P. & Bourque, C. W. An N-terminal variant of Trpv1 channel is required for osmosensory transduction. *Nat Neurosci* **9**, 93-98, doi:nn1614 [pii] 10.1038/nn1614 (2006).

[82] Xue, Q., Yu, Y., Trilk, S. L., Jong, B. E. & Schumacher, M. A. The genomic organization of the gene encoding the vanilloid receptor: evidence for multiple splice variants. *Genomics* **76**, 14-20, doi:10.1006/geno.2001.6582 S0888-7543(01)96582-6 [pii] (2001).

[83] Charrua, A. *et al.* Cystitis is associated with TRPV1b-downregulation in rat dorsal root ganglia. *Neuroreport* **19**, 1469-1472, doi:10.1097/WNR.0b013e32830f1e73 00001756-200810080-00005 [pii] (2008).

[84] Vos, M. H. *et al.* TRPV1b overexpression negatively regulates TRPV1 responsiveness to capsaicin, heat and low pH in HEK293 cells. *J Neurochem* **99**, 1088-1102, doi:JNC4145 [pii] 10.1111/j.1471-4159.2006.04145.x (2006).

[85] Smith, P. A., Moran, T. D., Abdulla, F., Tumber, K. K. & Taylor, B. K. Spinal mechanisms of NPY analgesia. *Peptides* **28**, 464-474, doi:S0196-9781(06)00554-7 [pii] 10.1016/j.peptides.2006.09.029 (2007).

[86] Moran, T. D., Colmers, W. F. & Smith, P. A. Opioid-like actions of neuropeptide Y in rat substantia gelatinosa: Y1 suppression of inhibition and Y2 suppression of excitation. *J Neurophysiol* **92**, 3266-3275, doi:10.1152/jn.00096.2004 00096.2004 [pii] (2004).

[87] Staaf, S., Oerther, S., Lucas, G., Mattsson, J. P. & Ernfors, P. Differential regulation of TRP channels in a rat model of neuropathic pain. *Pain* **144**, 187-199, doi:S0304-3959(09)00221-8 [pii]
10.1016/j.pain.2009.04.013 (2009).

[88] Brumovsky, P., Shi, T. S., Landry, M., Villar, M. J. & Hokfelt, T. Neuropeptide tyrosine and pain. *Trends Pharmacol Sci* **28**, 93-102, doi:S0165-6147(06)00286-0 [pii]
10.1016/j.tips.2006.12.003 (2007).

[89] Leslie, T. A., Emson, P. C., Dowd, P. M. & Woolf, C. J. Nerve growth factor contributes to the up-regulation of growth-associated protein 43 and preprotachykinin A messenger RNAs in primary sensory neurons following peripheral inflammation. *Neuroscience* **67**, 753-761, doi:0306-4522(95)00101-N [pii] (1995).

[90] Andersen, L. B. & Schreyer, D. J. Constitutive expression of GAP-43 correlates with rapid, but not slow regrowth of injured dorsal root axons in the adult rat. *Exp Neurol* **155**, 157-164, doi:S0014-4886(98)96903-5 [pii]
10.1006/exnr.1998.6903 (1999).

[91] Van der Zee, C. E. *et al.* Expression of growth-associated protein B-50 (GAP43) in dorsal root ganglia and sciatic nerve during regenerative sprouting. *J Neurosci* **9**, 3505-3512 (1989).

[92] Bennett, G. J. & Xie, Y. K. A peripheral mononeuropathy in rat that produces disorders of pain sensation like those seen in man. *Pain* **33**, 87-107 (1988).

[93] Baron, R. & Wasner, G. Complex regional pain syndromes. *Curr Pain Headache Rep* **5**, 114-123 (2001).

[94] Somers, D. L. & Clemente, F. R. Transcutaneous electrical nerve stimulation for the management of neuropathic pain: the effects of frequency and electrode position on prevention of allodynia in a rat model of complex regional pain syndrome type II. *Phys Ther* **86**, 698-709 (2006).

[95] Somers, D. L. & Clemente, F. R. Contralateral high or a combination of high- and low-frequency transcutaneous electrical nerve stimulation reduces mechanical allodynia and alters dorsal horn neurotransmitter content in neuropathic rats. *J Pain* **10**, 221-229, doi:S1526-5900(08)00737-2 [pii]
10.1016/j.jpain.2008.08.008 (2009).

[96] Somers, D. L. & Clemente, F. R. The relationship between dorsal horn neurotransmitter content and allodynia in neuropathic rats treated with high-frequency transcutaneous electric nerve stimulation. *Arch Phys Med Rehabil* **84**, 1575-1583, doi:S0003999303002909 [pii] (2003).

[97] Livak, K. J. & Schmittgen, T. D. Analysis of relative gene expression data using real-time quantitative PCR and the 2(-Delta Delta C(T)) Method. *Methods* **25**, 402-408, doi:10.1006/meth.2001.1262
S1046-2023(01)91262-9 [pii] (2001).

[98] Milligan, E. D. *et al.* Spinal glia and proinflammatory cytokines mediate mirror-image neuropathic pain in rats. *J Neurosci* **23**, 1026-1040, doi:23/3/1026 [pii] (2003).

[99] Davis, J. B. *et al.* Vanilloid receptor-1 is essential for inflammatory thermal hyperalgesia. *Nature* **405**, 183-187, doi:10.1038/35012076 (2000).

[100] Okabe, T., Sato, C., Matsumoto, K., Ozawa, H. & Sakamoto, A. Electroconvulsive stimulation (ECS) increases the expression of neuropeptide Y (NPY) in rat brains in a model of neuropathic pain: a quantitative real-time polymerase chain reaction (RT-PCR) study. *Pain Med* **10**, 1460-1467, doi:PME678 [pii] 10.1111/j.1526-4637.2009.00678.x (2009).

[101] Sommervaille, T., Reynolds, M. L. & Woolf, C. J. Time-dependent differences in the increase in GAP-43 expression in dorsal root ganglion cells after peripheral axotomy. *Neuroscience* **45**, 213-220, doi:0306-4522(91)90117-7 [pii] (1991).

[102] Ji, R. R., Samad, T. A., Jin, S. X., Schmoll, R. & Woolf, C. J. p38 MAPK activation by NGF in primary sensory neurons after inflammation increases TRPV1 levels and maintains heat hyperalgesia. *Neuron* **36**, 57-68, doi:S089662730200908X [pii] (2002).

[103] Facer, P. *et al.* Differential expression of the capsaicin receptor TRPV1 and related novel receptors TRPV3, TRPV4 and TRPM8 in normal human tissues and changes in traumatic and diabetic neuropathy. *BMC Neurol* **7**, 11, doi:1471-2377-7-11 [pii] 10.1186/1471-2377-7-11 (2007).

[104] Yu, L. *et al.* The role of TRPV1 in different subtypes of dorsal root ganglion neurons in rat chronic inflammatory nociception induced by complete Freund's adjuvant. *Mol Pain* **4**, 61, doi:1744-8069-4-61 [pii] 10.1186/1744-8069-4-61 (2008).

[105] Frederick, J., Buck, M. E., Matson, D. J. & Cortright, D. N. Increased TRPA1, TRPM8, and TRPV2 expression in dorsal root ganglia by nerve injury. *Biochem Biophys Res Commun* **358**, 1058-1064, doi:S0006-291X(07)00985-0 [pii] 10.1016/j.bbrc.2007.05.029 (2007).

[106] Michael, G. J. & Priestley, J. V. Differential expression of the mRNA for the vanilloid receptor subtype 1 in cells of the adult rat dorsal root and nodose ganglia and its downregulation by axotomy. *J Neurosci* **19**, 1844-1854 (1999).

[107] Maione, S. *et al.* Analgesic actions of N-arachidonoyl-serotonin, a fatty acid amide hydrolase inhibitor with antagonistic activity at vanilloid TRPV1 receptors. *Br J Pharmacol* **150**, 766-781, doi:0707145 [pii] 10.1038/sj.bjp.0707145 (2007).

[108] Casals-Diaz, L., Vivo, M. & Navarro, X. Nociceptive responses and spinal plastic changes of afferent C-fibers in three neuropathic pain models induced by sciatic nerve injury in the rat. *Exp Neurol* **217**, 84-95, doi:S0014-4886(09)00022-3 [pii] 10.1016/j.expneurol.2009.01.014 (2009).

[109] Dowdall, T., Robinson, I. & Meert, T. F. Comparison of five different rat models of peripheral nerve injury. *Pharmacol Biochem Behav* **80**, 93-108, doi:S0091-3057(04)00334-X [pii] 10.1016/j.pbb.2004.10.016 (2005).

[110] Robinson, I., Dowdall, T. & Meert, T. F. Development of neuropathic pain is affected by bedding texture in two models of peripheral nerve injury in rats. *Neurosci Lett* **368**, 107-111, doi:10.1016/j.neulet.2004.06.078 S0304-3940(04)00820-1 [pii] (2004).

[111] Kuphal, K. E., Solway, B., Pedrazzini, T. & Taylor, B. K. Y1 receptor knockout increases nociception and prevents the anti-allodynic actions of NPY. *Nutrition* **24**, 885-891, doi:S0899-9007(08)00292-X [pii] 10.1016/j.nut.2008.06.022 (2008).

[112] Shen, Y., Mani, S., Donovan, S. L., Schwob, J. E. & Meiri, K. F. Growth-associated protein-43 is required for commissural axon guidance in the developing vertebrate nervous system. *J Neurosci* **22**, 239-247, doi:22/1/239 [pii] (2002).

[113] Benowitz, L. I. & Routtenberg, A. GAP-43: an intrinsic determinant of neuronal development and plasticity. *Trends Neurosci* **20**, 84-91, doi:S0166-2236(96)10072-2 [pii] (1997).

[114] Verge, V. M., Tetzlaff, W., Richardson, P. M. & Bisby, M. A. Correlation between GAP43 and nerve growth factor receptors in rat sensory neurons. *J Neurosci* **10**, 926-934 (1990).

[115] Chong, M. S. *et al.* GAP-43 expression in primary sensory neurons following central axotomy. *J Neurosci* **14**, 4375-4384 (1994).

[116] Koltzenburg, M., Wall, P. D. & McMahon, S. B. Does the right side know what the left is doing? *Trends Neurosci* **22**, 122-127, doi:S0166-2236(98)01302-2 [pii] (1999).

[117] Kleinschnitz, C., Brinkhoff, J., Sommer, C. & Stoll, G. Contralateral cytokine gene induction after peripheral nerve lesions: dependence on the mode of injury and NMDA receptor signaling. *Brain Res Mol Brain Res* **136**, 23-28, doi:S0169-328X(05)00002-1 [pii] 10.1016/j.molbrainres.2004.12.015 (2005).

[118] Oaklander, A. L. & Belzberg, A. J. Unilateral nerve injury down-regulates mRNA for Na+ channel SCN10A bilaterally in rat dorsal root ganglia. *Brain Res Mol Brain Res* **52**, 162-165, doi:S0169328X97002398 [pii] (1997).

[119] Mosavi, L. K., Cammett, T. J., Desrosiers, D. C. & Peng, Z. Y. The ankyrin repeat as molecular architecture for protein recognition. *Protein Sci* **13**, 1435-1448, doi:10.1110/ps.03554604 13/6/1435 [pii] (2004).

[120] Sedgwick, S. G. & Smerdon, S. J. The ankyrin repeat: a diversity of interactions on a common structural framework. *Trends Biochem Sci* **24**, 311-316, doi:S0968-0004(99)01426-7 [pii] (1999).

[121] Hellwig, N., Albrecht, N., Harteneck, C., Schultz, G. & Schaefer, M. Homo- and heteromeric assembly of TRPV channel subunits. *J Cell Sci* **118**, 917-928, doi:jcs.01675 [pii] 10.1242/jcs.01675 (2005).

[122] Huang, J., Zhang, X. & McNaughton, P. A. Modulation of temperature-sensitive TRP channels. *Semin Cell Dev Biol* **17**, 638-645, doi:S1084-9521(06)00114-5 [pii] 10.1016/j.semcdb.2006.11.002 (2006).

[123] Obreja, O., Rathee, P. K., Lips, K. S., Distler, C. & Kress, M. IL-1 beta potentiates heat-activated currents in rat sensory neurons: involvement of IL-1RI, tyrosine kinase, and protein kinase C. *FASEB J* **16**, 1497-1503, doi:10.1096/fj.02-0101com

16/12/1497 [pii] (2002).
124 Ma, W., Zhang, Y., Bantel, C. & Eisenach, J. C. Medium and large injured dorsal root ganglion cells increase TRPV-1, accompanied by increased alpha2C-adrenoceptor co-expression and functional inhibition by clonidine. *Pain* **113**, 386-394, doi:S0304-3959(04)00555-X [pii] 10.1016/j.pain.2004.11.018 (2005).
125 Amaya, F. *et al.* Local inflammation increases vanilloid receptor 1 expression within distinct subgroups of DRG neurons. *Brain Res* **963**, 190-196, doi:S0006899302039720 [pii] (2003).
126 Vazquez, E. & Valverde, M. A. A review of TRP channels splicing. *Semin Cell Dev Biol* **17**, 607-617, doi:S1084-9521(06)00118-2 [pii] 10.1016/j.semcdb.2006.11.004 (2006).
127 Winston, J., Toma, H., Shenoy, M. & Pasricha, P. J. Nerve growth factor regulates VR-1 mRNA levels in cultures of adult dorsal root ganglion neurons. *Pain* **89**, 181-186, doi:S0304395900003705 [pii] (2001).
128 Gong, H. *et al.* Effects of selective alpha 2-adrenoreceptor stimulation on capsaicin-evoked substance P release from primary cultured dorsal root ganglion neurons. *Pharmazie* **65**, 202-205.